Journal of Structural Geology, Vol. 14, No. 7, pp. 807 to 823, 1992
Printed in Great Britain

0191-8141/92 $05.00+0.00

Variscan shear-zone deformation of late Precambrian basement in SW Iberia: implications for circum-Atlantic pre-Mesozoic tectonics

BENITO ABALOS

Dep. de Estratigrafía, Geodinámica y Paleontología, Univ. del País Vasco, P.O. Box 644, E-48080 Bilbao, Spain

(*Received* 28 *August* 1991; *accepted in revised form* 24 *February* 1992)

Abstract—Polyphase deformation and metamorphism in the Badajoz–Córdoba Shear Belt (SW Spain) relate to a poly-orogenic evolution involving two major tectonothermal episodes: the accretion of mid- and lower-crust tectonic slices in an orogenic wedge complex during pre-Variscan times, and the development of an intracontinental ductile shear zone during the late Palaeozoic. Structural analysis of zones with different intensities of shear-dominated Variscan deformation allows a recognition of the poly-deformed nature of most units of the belt, identification of varying deformation mechanisms, and a description of the geometry of early structures. The implications for the regional tectonics of this area of the southern Iberian Massif are discussed in the light of the geodynamic evolution of the Ibero-Armorican arc during the Variscan orogeny and the reconstruction of the late Precambrian Cadomian–Avalonian–Panafrican orogen of the circum-Atlantic region.

INTRODUCTION

THE directions of relative tectonic movements between convergent plates, and orientation of the edges of opposite continental margins, play a crucial role during lithospheric oblique convergence and continental collision processes. In transpressive orogens, orientation of both plate convergence vectors and zones of tectonic movement (often bands of weakened crust) govern the kinematic partitioning of the lithospheric convergence vector into transverse, oblique and parallel movement zones. Suture zones are complex crustal-scale tectonic movement zones that accommodate components of such large displacements between crustal blocks. Many factors constraining their geodynamic evolution during oblique plate convergence (Buck & Tocksöz 1983) lead to the creation of zones of weakened crust that enable decomposition of tectonic convergence vectors during the subsequent evolution of mountain belts. In recent years, the importance of orogen-parallel tectonic motions has been realized and has led to new perspectives of mountain-building processes; in particular, the importance of the third dimension in geodynamic models (Sengör 1991). This new viewpoint focuses on the ubiquity of large-scale tectonic displacements along strike, as recognized in mountain belts of different ages in several parts of the world (Vauchez & Nicolas 1991).

In the context of the European Hercynides the Badajoz–Córdoba Shear Zone (BCSZ) of the southern Iberian Massif has been considered by many authors as a suture and/or a left-lateral intracontinental shear zone accommodating large displacements between the blocks separated to the northeast and southwest (Burg *et al.* 1981, Matte 1991, among others). However, in spite of some consideration in large-scale tectonic models, the belt remains poorly known in several ways, including its detailed structure and geodynamic evolution.

In this paper new data concerned with the structural analysis of superimposed deformations in the BCSZ are presented. Polyphase deformation and metamorphism relate to a poly-orogenic evolution of the belt including two major tectonothermal episodes: (1) the accretion of mid- and lower-crust tectonic slices in an orogenic wedge complex (regional D_1) during pre-Variscan times (Cadomian s.l. orogeny; latest Precambrian–early Palaeozoic); and (2) the development of an intracontinental ductile shear zone during the Variscan orogeny (regional D_2 and D_3; late Palaeozoic).

These tectonic events are characterized by distinctive structures and kinematic patterns. However, recognition of the oldest structures is hampered by the pervasive character of Variscan deformations, which reorientate and usually erase them. The central part of the BCSZ will be described for the Hornachos area of SW Spain (Figs. 1 and 2). Structural analysis of zones with different intensities of Variscan deformation (sinistral wrenching under ductile through brittle conditions) will reveal the poly-deformed nature of most units of the belt, will identify varying deformation mechanisms, and will describe the geometry of early structures.

The implications for the regional tectonics of this area are then discussed in the light of the Variscan geodynamic evolution of the Ibero-Armorican arc and the reconstruction of the Cadomian–Avalonian–Panafrican orogen of the circum-Atlantic region. In both cases several tens of kilometres of strike-parallel horizontal displacements took place, highlighting the importance of orogen-parallel displacements during mountain building.

GEOLOGICAL SETTING

The BCSZ is a 30–40 km wide and 400 km long structure that extends in the Iberian Peninsula through Portugal and SW Spain. The shear zone trends NW–SE

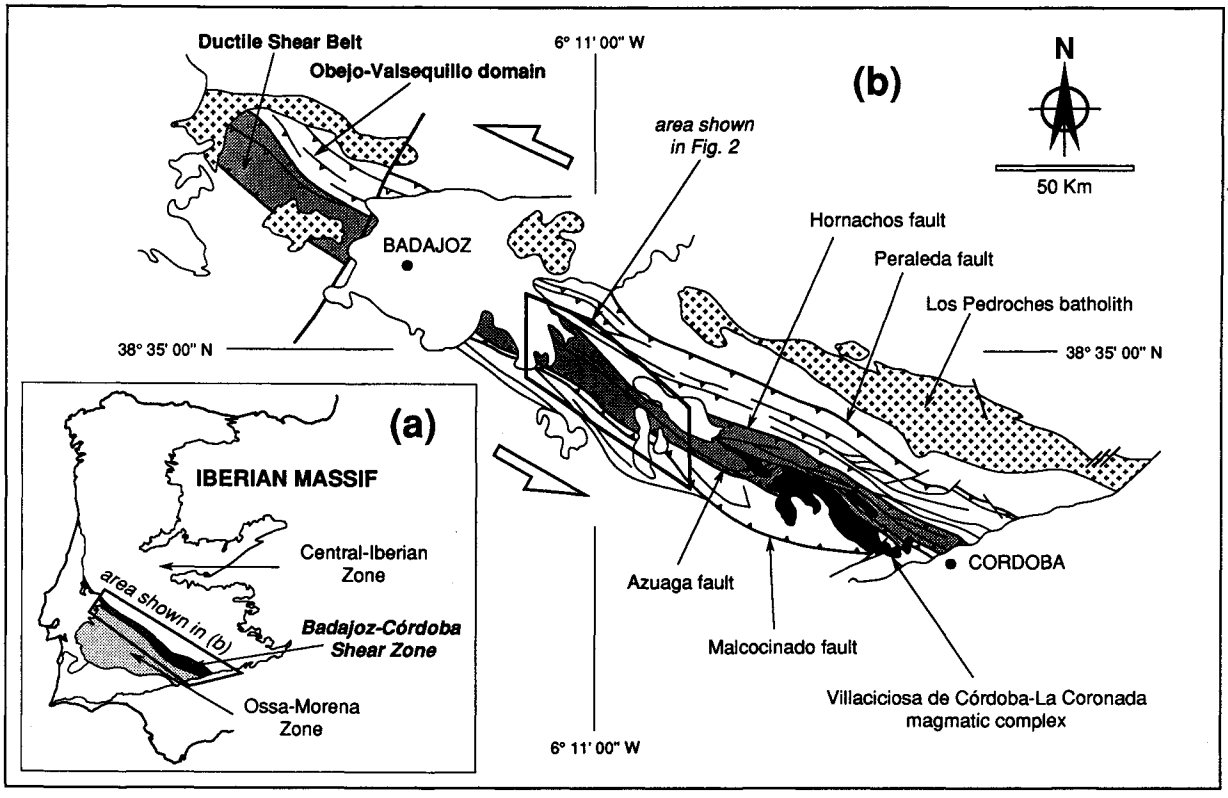

Fig. 1. (a) Sketch of the Iberian Massif. (b) Geological sketch map of the fault-bounded Badajoz–Córdoba Shear Zone, in SW Spain.

and is bounded by the Peraleda and Malcocinado faults (Fig. 1). The BCSZ is composed of late Precambrian metamorphic rocks unconformably overlain by distinctive Palaeozoic successions. The late Precambrian 'Serie Negra' crops out widely all over the BCSZ. However, the Hornachos fault separates two distinctive lower Palaeozoic palinspastic domains with different stratigraphic records, faunas and palaeogeographic histories (Paris & Robardet 1977): the Obejo–Valsequillo domain to the northeast (with the Serie Negra unconformably overlain by early Ordovician quartzites; Apalategui & Pérez-Llorente 1983) and the 'Ductile Shear Belt' to the southwest (Fig. 1). The latter belt comprises a late Precambrian basement (Serie Negra and associated units) unfonformably overlain by latest Precambrian to earliest Cambrian volcano-sedimentary and molassic sequences (Quesada 1990 and references therein).

Whilst so far the 'Ductile Shear Belt' has received several designations from different schools (e.g. Bladier 1974, Laurent 1974, Burg *et al.* 1981, Mata & Munhá 1986, Abalos 1990 and references therein) in the present paper the term 'Badajoz–Córdoba Ductile Shear Belt' or simply 'Ductile Shear Belt' (DSB) will be used. The DSB extends NW–SE for more than 300 km with an average width in the range 5–15 km (Fig. 1b). It is principally composed of mylonitic rocks and constitutes a narrow zone of transcurrent Variscan deformation. The occurrence of high-pressure rocks and the pervasive ductile deformation (coeval with greenschist- and amphibolite-facies metamorphism) are the features that have led many authors to consider the DSB to be a Variscan suture where the high-grade complexes of NW Iberia were rooted (Matte 1991). Recent works concerned with field geology and progress in geochronology (Dallmeyer & Quesada 1989, Schäfer *et al.* 1989, Quesada *et al.* 1990, Schäfer 1990) have constrained the geodynamic evolution of the DSB. The tectonic evolution of the DSB occurred in two superimposed orogenic episodes: the building of a pre-Variscan subduction–collision orogenic wedge complex (D_1 event, late Precambrian–early Palaeozoic), and its reworking under transpression from ductile (D_2) through brittle (D_3) conditions during Variscan intracontinental shearing.

LITHOSTRATIGRAPHY AND FIELD RELATIONSHIPS OF THE DUCTILE SHEAR BELT (DSB)

Lithostratigraphy

In the Hornachos area (Fig. 2) the DSB is characterized by a thick (5–10 km) allochthonous pile of late Precambrian medium- to high-grade metamorphic rocks emplaced onto a para-autochthonous low-grade metapelitic sequence (Atalaya Schist and Azuaga Formations) of uncertain age between the latest Precambrian and the early Palaeozoic (early Cambrian?). The allochthonous pile consists of five slices separated by 10–100 m thick mylonitic–ultramylonitic bands. High-pressure and high-grade metamorphism in these units (M_1) was synchronous with D_1. From the base to the top of the

pile the following units are distinguished (Abalos 1990, Abalos *et al.* 1991a).

The Higuera de Llerena mylonite gneiss is at least 400–500 m thick and is composed of high-grade garnet–sillimanite–biotite-bearing augen gneisses with relicts of kyanite. The gneisses become finer-grained upwards, resulting in a 100–200 m thick ultramylonite band. Whilst the maximum *P–T* conditions recorded in this unit during M_1 were 720 ± 30°C and 800 ± 50 MPa, an evolution towards lower pressure (730 ± 50 MPa) and temperature (≈660 ± 30°C) has been inferred.

The blastomylonitic slice of migmatitic gneisses is a 3–4 km thick unit consisting of migmatitic biotite–garnet–sillimanite-bearing paragneisses, anatectic leucocratic mobilisates, orthogneisses, and garnet–amphibolite and eclogite layers. These rocks were affected by pervasive D_2 blastomylonitic deformations and are cross-cut by a large amount of late ultramylonitic bands. The biotite-rich migmatitic gneisses underwent peak metamorphic conditions during M_1 at ≈670 ± 30°C and 1000 ± 50 MPa and then evolved towards lower pressures (670 ± 50 MPa) and temperatures (≈610 ± 30°C). The leucocratic gneisses (probably anatectic mobilisates) record distinctly lower *P–T* conditions, from ≈520 ± 30°C at 640 ± 50 MPa to 510 ± 30°C at 530 ± 50 MPa.

The eclogitic slice consists of garnet amphibolites (locally 500 m thick) carrying lenticular masses of variably retrogressed gneisses, ultramafic rocks and eclogites. The gabbroic protolith of the eclogites has been dated at 611 +17/−12 Ma (U–Pb in zircon; Schäfer 1990). *P–T* conditions for eclogites (peak M_1) have been estimated at ≈685 ± 25°C and >1500 MPa. The retrograde *P–T* path involved various stages of retrogression with a continuous decrease in pressure and an increase in temperature from ≈680 ± 25°C and 1150 ± 50 MPa to ≈770 ± 25°C and 600 ± 100 MPa. Whilst retrogressed eclogites were subjected to ≈580 ± 25°C and 900–1100 MPa, garnet-amphibolites lacking eclogite relicts record lower-grade *P–T* conditions of ≈500 ± 25°C and 600–800 MPa.

The leptino-amphibolic unit consists of felsic gneisses, alkali orthogneisses and amphibolites with minor calc-silicate rocks and quartzites. Mineral assemblages and *P–T* estimates from this unit are typical of intermediate-pressure amphibolite-facies M_1.

The Serie Negra is the uppermost metasedimentary unit. This is a thick and homogeneous low- to medium-grade metapelitic succession containing black quartzites, meta-greywackes and epidote–amphibolite layers. At the base of the unit migmatitic rocks occur locally (Mina Afortunada gneiss dome area; Fig. 2), *P–T* estimates are consistent with greenschist- and amphibolite-facies M_1 with local anatexis at 650°C and 600–700 MPa.

The metapelitic para-autochthon of the DSB is exposed in three bands (Fig. 2) which from the southwest to the northeast are as follows: (1) the band embraced by the Malcocinado and Azuaga faults; (2) the Ribera del Fresno tectonic window; and (3) the Atalaya window (the band where the Atalaya Formation crops out). M_1 mineral assemblages yield 500–550°C at 200–300 MPa at upper structural levels near the basal thrust of the allochthonous stack (Azuaga Formation) and 500–575°C and 700–900 MPa in the deepest structural levels beneath (Atalaya Formation). A scheme of 'inverted metamorphism' with respect to the allochthonous stack is remarkable, a *P* gradient existing SW–NE from the upper (where pressures of *ca* 300–400 MPa are dominant) to the lowermost structural levels (with intermediate and relatively high pressure prevailing; cf. Abalos 1990).

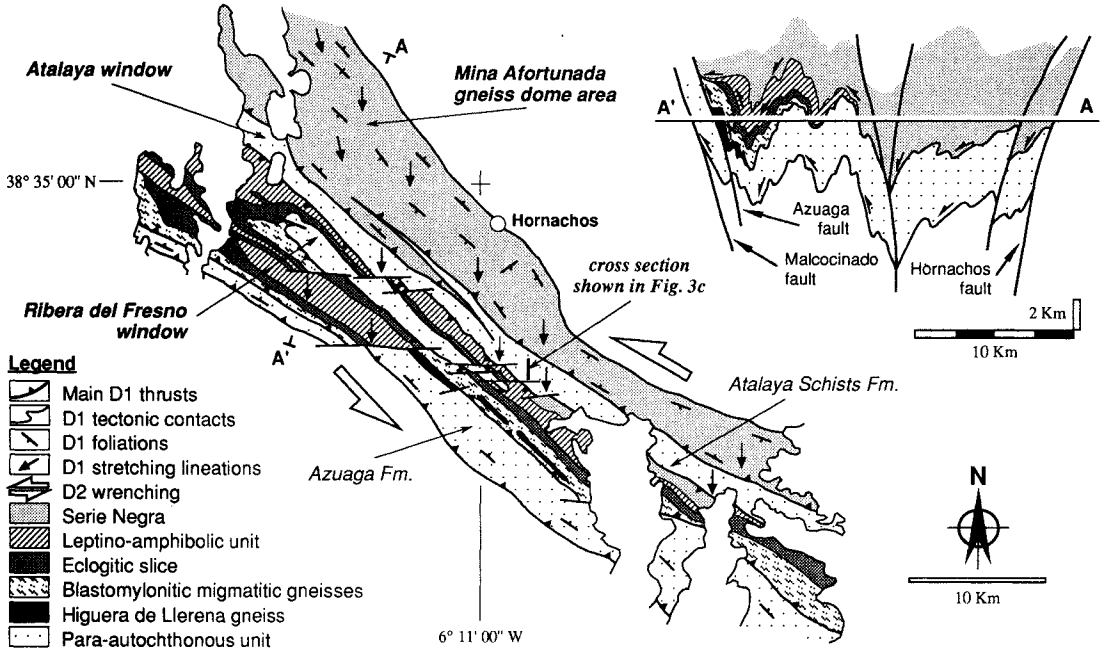

Fig. 2. Geological map and schematic cross-section for the central part of the Ductile Shear Belt.

Field relations and the relative chronology of deformations

The Atalaya window separates two areas in which different units of the allochthonous stack are exposed (Fig. 2). Whilst northeast of this structure the Serie Negra is the only tectonic slice of the allochthonous pile that crops out, to the southwest occasional outcrops of the Serie Negra exist, and the four basal gneissic slices crop out widely.

The Atalaya Formation is intruded by pre-Variscan orthogneisses emplaced at about 200–300 MPa and 700–800°C (Abalos 1990) and dated *ca* 632 + 192/−74 Ma (U–Pb in zircon; Schäfer 1990). García Casquero *et al.* (1985) reported an 'intrusion' age of 423 ± 38 Ma (Rb–Sr on whole rock), whereas a 330–335 Ma cooling age ($^{40}Ar/^{39}Ar$ on biotite) related to the pervasive D_2 ductile deformation was obtained by Blatrix & Burg (1981). This intrusive post-dates D_1 and M_1, as evidenced by: (1) orthogneiss dykes cross-cutting D_1 foliations in the metapelitic para-autochthon; (2) metapelitic xenoliths in the gneiss with D_1 fabrics; and (3) misoriented garnet and biotite neoblasts sealing S_1 in biotite-rich layers (static microtextures related to contact metamorphism post-dating the D_1 schistosity in country rock metapelites). S_1 and contact metamorphism structures are largely affected by folds, crenulations, schistosity boudinage, development of shear planes (S_2 schistosity) and C' surfaces in the most strained zones. The chronology of D_1 should be considered Cadomian s.l., this age being in agreement with other events recognized in neighbouring areas of the Ossa–Morena (Quesada 1990).

The whole stack of autochthonous and allochthonous units underwent intense sinistral shearing during an episode of low cooling rate, from 360–368 ± 3 Ma ($^{40}Ar/^{39}Ar$ in hornblende) to 331–340 ± 1 Ma ($^{40}Ar/^{39}Ar$ in muscovite; Dallmeyer & Quesada 1989), these ages being the same range as those reported by García Casquero *et al.* (1988). The widespread low- to medium-grade M_2 metamorphism may be associated with such late Devonian to early Carboniferous shear zone ductile deformation. These episodes are post-dated by unconformable volcano-sedimentary series and by the intrusion of sub-volcanic igneous complexes of Visean age (Fig. 1).

SUPERIMPOSED DEFORMATIONS IN THE DSB

The nature of Variscan deformations is quite different at both sides of the Atalaya window, early structures being dominant to the northeast of the area, and pervasive Variscan ductile deformations transposing previous structures to the southwest. In the area southwest of the Atalaya window there exist passive markers (the Ribera del Fresno gneiss) subjected only to Variscan deformations that enable the recognition and separation of late Palaeozoic structural features. Northeast of the Atalaya window inspection of oriented thin sections and the use of techniques of conventional structural analysis enable recognition of the geometry and kinematics of superimposed deformations.

Geometry and kinematics of D_1 *structures*

In the area southwest of the Atalaya window S_1 occur only in pods of high-grade blastomylonitic rocks surrounded by D_2 mylonitic foliations. In high-grade gneisses and in some garnet amphibolites S_1 appears as oriented inclusions of quartz and opaques within pre-D_2 garnet porphyroclasts, whilst in eclogites rutile–ilmenite bands and retrogressed granoblastic garnet–omphacite textures define S_1. After allowing for the effects of Variscan overprinting, penetrative synmetamorphic S_1 was approximately parallel with D_1 tectonic contacts. In upper units of the allochthon, S_1 foliations with prominent stretching lineations (L_1) which trend N160–200E are locally recognized (Fig. 2). These lineations are outlined in gneisses by the elongation of feldspars, quartz ribbons and mica aggregates. Shear criteria related to the scarce D_1 structures determined in the field and in thin sections (*S–C* structures and sigmoidal porphyroclast systems) provide a consistent pattern of S-vergent shear.

In the Atalaya window, large, recumbent, southward-vergent D_1 folds with an axial planar S_1 characterize the structure of the para-autochthonous rocks. S_1 ranges from a slaty cleavage to a schistosity in the proximity of the basal thrust of the allochthonous stack. N–S-trending, L_1 stretching lineations are locally found near this thrust, where the geometry of recumbent folds (N160E-trending) and the respective stratigraphic way-up criteria imply south-southwestwards vergence (Fig. 3c). Whilst D_1 structures from most of the para-autochthon (mainly apart from the basal thrust of the allochthon) characterize a deformation regime of combined simple shear and flattening, some structures in the proximity of the basal thrust enable the identification of non-coaxial deformation increments. Shear-sense criteria related to D_1 determined in the field (asymmetry of sheath and *-a-* type folds) and in thin sections denote S-vergent shear.

In the area northeast of the Atalaya window a S_2 tectonic banding crenulates and even transposes the earlier S_1 cleavage preserved as relict graphite and biotite alignments inside porphyroblasts or microlithons. Penetrative, subhorizontal, S_1 was parallel to the main tectonic contacts before D_2. N–S-trending (N160–200E) L_1 stretching lineations are locally recognized (Figs. 2 and 4). They are outlined by the elongation of feldspars, quartz ribbons and mica aggregates in migmatites, and by the elongation of quartz grains and graphite aggregates in quartzites. Occasional m-scale recumbent, southward-vergent D_1 folds are found near the contact of this unit with the para-autochthon (Fig. 4g). Structures of the upper parts of the Serie Negra characterize a deformation history of combined simple shear and non-coaxial strain. Shear-sense criteria related to D_1 structures include the sigmoidal disposition of S_1 schistosity, asymmetry of sheath and *-a-* type folds, *S–C* structures

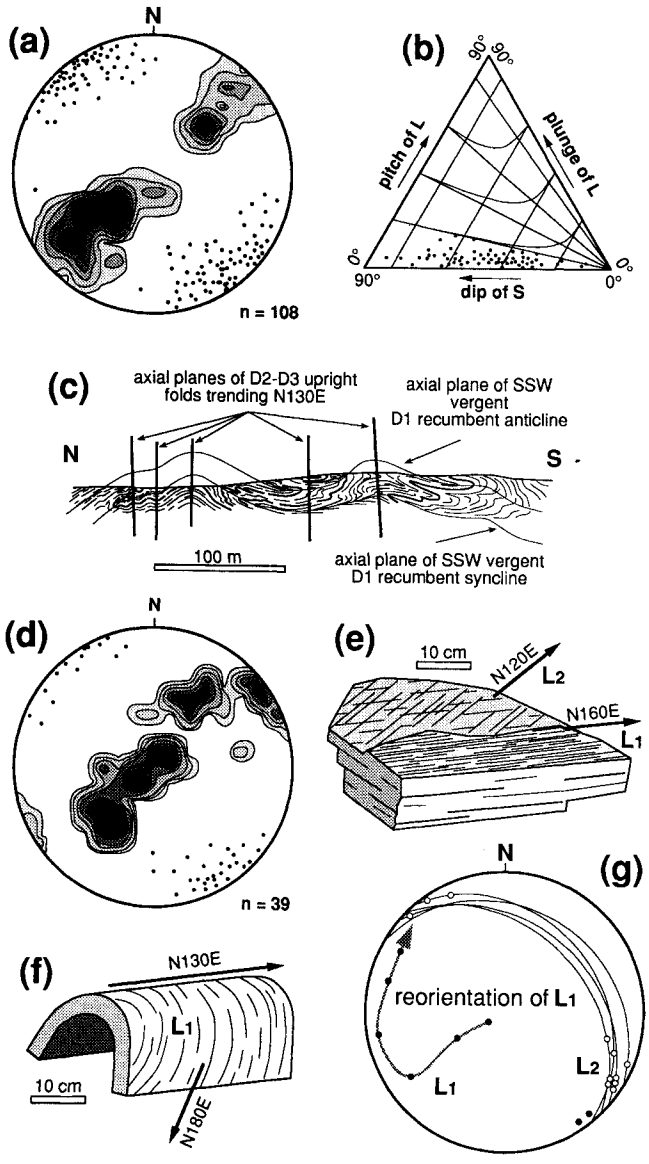

Fig. 3. Structural elements and orientation diagrams for the structures observed in the Atalaya window. (a) Equal-area, lower-hemisphere stereoplot for S_1 and S_2 foliations (contour intervals 1%) and L_1+L_2 lineations (dots). (b) Diagram showing the relative evolution of the S_2 plane dip and the pitch/plunge of L_2. (c) Near N–S cross-section of the central part of the Atalaya window (see location in Fig. 2) showing the geometry of recumbent D_1 folds and superimposed Variscan upright folds. (d) Equal-area, lower-hemisphere stereoplot for the axial planes of D_1 recumbent folds (contour intervals 1%) and their fold-axes (dots). (e) Sketched block representative of areas with steeply dipping foliations in which the clear superposition of L_1 and L_2 with distinct orientations is observed. (f) Sketch of a D_2 fold representative of shallow dipping areas in which L_1 stretching lineations are folded and reoriented without superposition of D_2 penetrative structures. (g) Equal-area, lower-hemisphere stereoplot of reorientation of L_1 'hairpins' towards the trends of D_2 structures (S_2 planes: major circles; open dots: L_2 lineations) as sketched in (f).

and sigmoidal porphyroclast systems. They consistently denote S-vergent shear. In upper structural levels of the Serie Negra rotational components related to D_1 are less evident, suggesting a coaxial deformation history.

Geometry and kinematics of D_2 *structures*

In the area southwest of the Atalaya window Variscan reworking of the Cadomian basement is polyphase and complex. The observed structures are consistent with ductile shearing under temperature conditions evolving with time from the amphibolite to the lower greenschist facies. The deformational microstructures observed can be described in terms pertinent to mylonitic rocks. These rocks have a well developed *S–L* fabric. Formation of an S_2 gneissic foliation almost completely obliterated previous structures. Stretching and mineral L_2 are outlined by elongation of feldspar porphyroclasts, quartz ribbons and mica aggregates in pelitic gneisses and by parallel orientation of amphibole and plagioclase aggregates in metabasites. Porphyroclast systems of the types 'sigma' and 'delta', sigmoidal pressure-shadows, *S–C* structures, mica-fish, obliquities between quartz sub-boundaries and quartz ribbon elongations, etc. (cf. Bouchez *et al.* 1983, Simpson & Schmid 1983, Lister & Snoke 1984, Passchier & Simpson 1986) are good shear-sense indicators that confer an *S–C*-type mylonitic fabric to most of these rocks. The geometry of *S–C* microstructures, asymmetric pressure shadows and mica-fishes is often obliterated as a shear-sense indicator, at increased strain, because of grain-size reduction. Microstructures indicate non-coaxial deformation of variable intensity. All the shear-sense criteria available provide a consistent and ubiquitous pattern of sinistral wrenching.

In the Atalaya window Variscan deformations gave rise to the development of NW–SE-trending (N135E), upright, open folds with local axial planar S_2 rough slaty cleavage or crenulation cleavage. Folding of S_0+S_1 planes during D_2 gave rise to Ramsay's (1967) type-3 interference patterns at different scales (Fig. 3). Several varieties of lineation types occur on the folded S_1 surfaces: intersection and microfolding-crenulation lineations between S_2 cleavage and S_1 schistosity, and local stretching lineations. Whilst the former are essentially parallel to D_2 fold axes (Figs. 3a & d, respectively), the latter are shallow plunging and occur mostly on steeply dipping cleavage planes. When observed in *XZ* thin sections (with *XY* planes = S_2 cleavage; *X* direction = L_2 stretching lineation), rocks with steeply dipping cleavage exhibit *S–C* microstructures and spaced S_2 shears that result in megascopic composite foliations. 'Snowball' garnets often form asymmetric porphyroclast systems whose external morphology and internal organization denote a deformation regime of localized simple shear during D_2. These shear-sense indicators and the orientations of L_2 stretching lineations are consistent with sinistral wrenching.

In the area northeast of the Atalaya window, gneissic rocks cropping out in the Mina Afortunada dome area (see Fig. 2) are D_2 tectonites with a well developed S_2–L_2 fabric resulting from mylonitization of granodiorites and migmatites with D_1 fabrics. Non-coaxial deformation of variable intensity is indicated by various microstructures (sigmoidal pressure-shadows, 'sigma' and 'delta' porphyroclast systems, *S–C* structures, obliquities between quartz sub-boundaries and quartz ribbon elongations, etc.). Heterogeneous S_2 tectonic banding and crenulation cleavage is widespread in pelitic lithologies of the Serie Negra. At the scale of thin

section, rock volumes affected by progressive shortening are adjacent to anastomosing zones affected by progressive shearing. Bulk inhomogeneous shortening, probably driven by deformation partitioning as described by Bell & Rubenach (1980), might account for the observed features. However, L_2 in the Serie Negra are not always intersection lineations between S_1 and S_2 but stretching lineations. Substantial shearing along S_2 is thus expected to accompany bulk shortening. S_2 foliations and L_2 stretching lineations in both fine- and coarse-grained metabasites (defined by preferred orientation of amphiboles and compositional layering) are often associated with discrete shear zones parallel to the D_2 regional trend (N135E).

Structural analysis of S–L *orientation data*

In the area southwest of the Atalaya window, the *S–C* orthogneisses cropping out in the Ribera del Fresno window (Fig. 2) record only the deformation phase responsible for the development of the widespread *S–C* fabrics (D_2). *C* planes (the megascopic foliation, here labelled S_2) are variably dipping N135E-striking surfaces parallel with S_2 planes of the allochthonous rocks surrounding the gneiss (Fig. 5a). The L_2 stretching lineations, measured on the *C* planes, are subhorizontal (0–20°) and their orientation all over the gneiss outcrop is in the range N130–160E. The plunge of L_2 varies slightly along strike (Fig. 5c). The relative evolution of L_2 plunge with respect to the dip of S_2 planes is represented in Fig. 5(b). Points plotted on the triangular diagram exhibit a continuous variation from apparent thrust- to wrench-type relationships through intermediate situations. As suggested by the persistence of shear-sense criteria and the shallow plunge of L_2 all over the Ribera del Fresno gneiss, the L_2–S_2 relationships can be explained by means of a single episode of ductile deformation resolving sinistral wrenching on variably dipping N135E shear planes. In the medium- and high-grade rocks surrounding the Ribera del Fresno gneiss, the N130–150E-trending S_2 is usually steeply dipping (Fig. 5d). The relationship between L_2 plunge and S_2 dip (Fig. 5e) show a roughly continuous variation from apparent thrust- to dominant wrench-type relationships consistent with sinistral wrenching. Intermediate situations with shallow plunging L_2 imply the onset of wrenching on gently dipping S_2. Since no regular relationship has been observed in the field between the variation of S_2 strike and the plunge of L_2 in outcrops where L_2 plunges more than 20–30°, interaction between lateral and frontal thrust ramps does not explain satisfactorily the occurrence of steeply dipping planes with steeply plunging

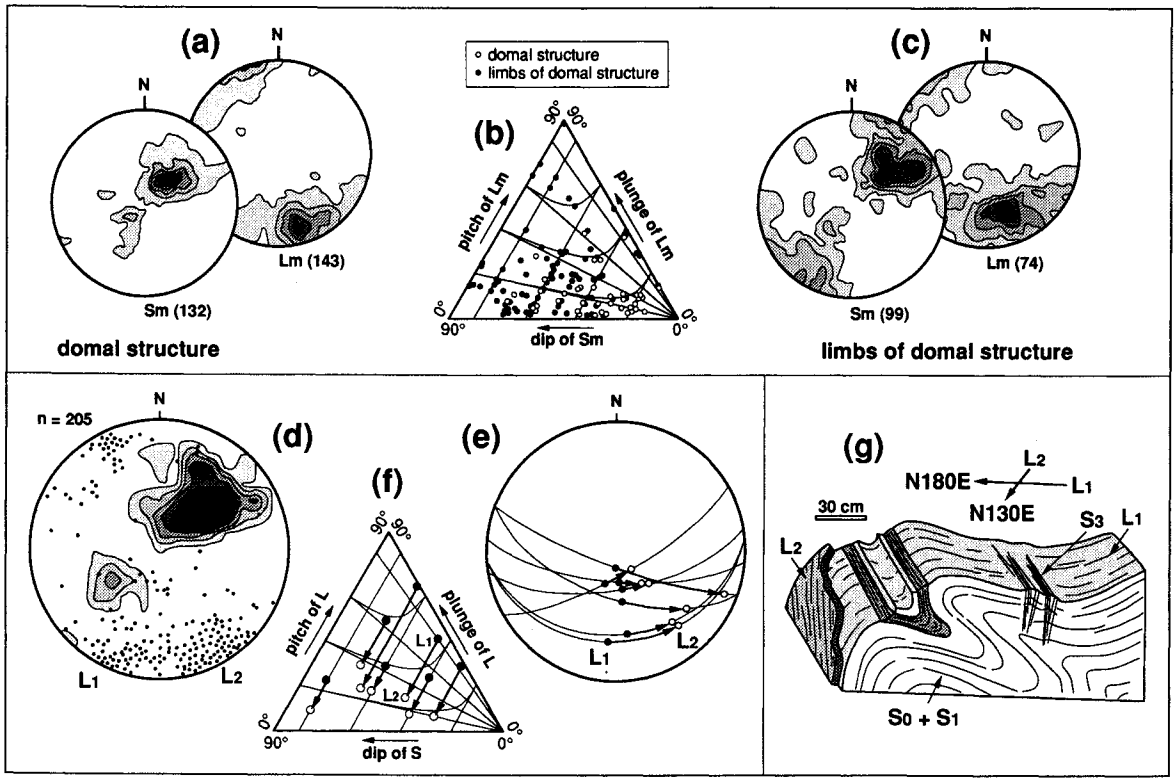

Fig. 4. Structural elements and orientation diagrams for the structures observed in the area northeast of the Atalaya window. (a) Equal-area, lower-hemisphere stereoplots for S_2 and L_2 in areas with gently dipping foliations (contour intervals 1.5%). (b) Triangular diagram showing the geometrical relationship between the plunge of D_2 mylonitic lineations (Lm) and the dip of D_2 mylonitic foliations (Sm) in areas with gently and steeply dipping foliations. (c) Plot as (a) but in areas with steeply dipping foliations (contour intervals 1.5%). (d) Equal-area, lower-hemisphere stereoplot for S_2 (contours) and L_1+L_2 (dots), in areas with superimposed structures (contour intervals 1%). (e) Equal-area, lower-hemisphere stereoplot illustrating reorientation of L_1 towards the trends of L_2. (f) Triangular diagram illustrating reorientation of D_1 structures (black dots) towards D_2 trends (open dots) through the geometrical relationships between the plunge of lineations (*L*) and the dip of foliations (*S*). (g) Schematic block diagram showing the geometry of D_1, D_2 and D_3 structures in a single outcrop near the basal thrust of the allochthonous unit.

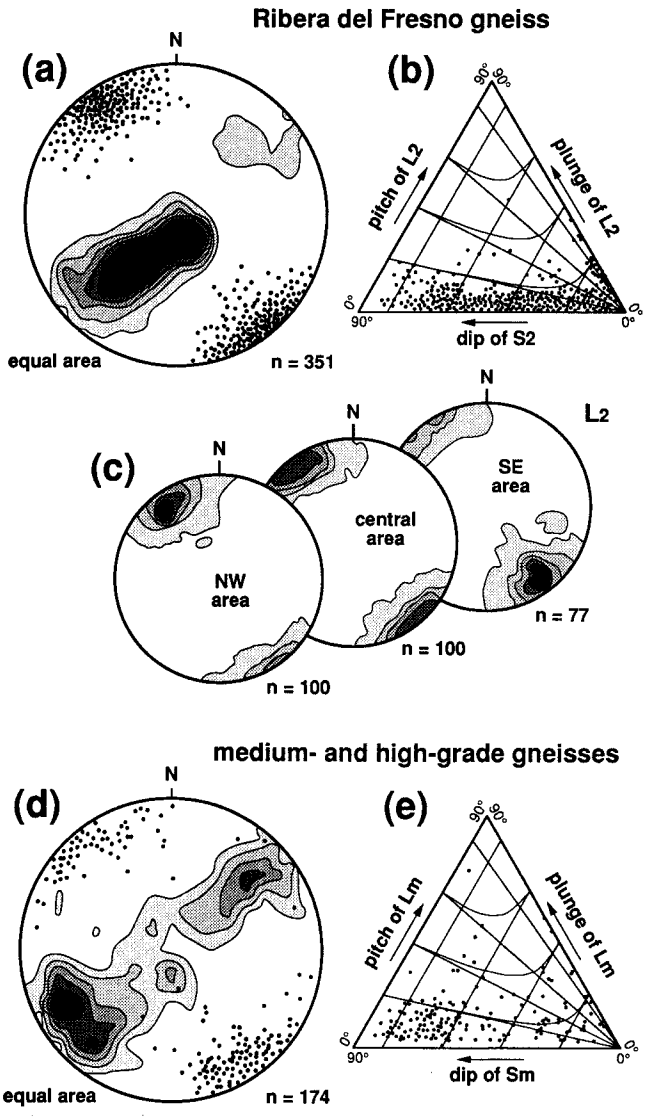

Fig. 5. Structural elements and orientation diagrams for the structures observed in the area southwest of the Atalaya window. Ribera del Fresno gneiss. (a) Equal-area, lower-hemisphere stereoplot for regional S_2 (S–C foliations, contour intervals 1%) and L_2 (dots). (b) Diagram showing the relative evolution of the S_2 plane dip and the pitch or plunge of L_2. (c) Equal-area, lower-hemisphere stereoplots for the variation of L_2 plunge in the Ribera del Fresno window (contour intervals 2%). Medium- and high-grade gneisses. (d) Equal-area, lower-hemisphere stereoplot for D_2 mylonitic foliations (contour intervals 1%) and stretching lineations (dots). (e) Diagram showing the relative evolution of D_2 mylonitic foliation (Sm) dip and the pitch or plunge of corresponding stretching lineations (Lm).

lineations. Whilst the observation in the field of L_1 and L_2 on the same foliation plane is very unusual, when they occur together L_1 shows large pitch angles whereas L_2 is near parallel with the strike of S_2. Steeply dipping and plunging structures could be due to partial reorientation without transposition of L_1 towards the trend of D_2.

In the Atalaya window, analysis of structural orientation data requires consideration of two distinct zones whose scale may be metric to decametric: areas with gently dipping S_1 on one side, and areas with steeply dipping S_1 on the other. Differentiation of these two domains is of great interest since accommodation of D_2 is governed by strain partitioning into them. In the former areas mainly S_1 axial plane foliations and L_1 stretching lineations related to recumbent folds occur. Lineations are often reoriented and deformed by open D_2 upright folds (see Figs. 3f & g) and their orientation, initially close to N–S, is progressively overturned to the axial trends of D_2 (N135E). Occurrence of both D_1 and D_2 structures in the same outcrop is restricted to superposition of subvertical S_2 crenulation cleavages on subhorizontal S_1 schistosity. In the limbs of D_2 folds new S_2 and L_2 form with a N135E–140E trend. The dip of composite S_2 ranges between 30° and 70° and the plunge of L_2 on them is often 20° or less (Figs. 3a & b). This geometric organization and the deformation regime and shear-sense indicators point to sinistral wrenching on N135E shear planes dipping 30–70°. Superposition of D_1 and D_2 structures and strain partitioning at the scale of hand specimens may be observed in these domains (Fig. 3e). Some quartzo-feldspathic beds contain superimposed L_1 (penetrative) and L_2 (spaced). Here, orientation of steeply plunging L_1 is close to N–S (when the plane that contains it is tilted to the horizontal), whereas shallow plunging L_2 trends NW–SE.

In the area northeast of the Atalaya window regional D_2 is characterized by alternating areas of shallow and steeply dipping foliations (see Figs. 4a & c). Areas with shallow dipping foliations (such as the Mina Afortunada dome) are characterized by oblique and transverse L_2 (with strikes in the range N160–230E), whereas the steeply dipping areas have more or less N135–140E trending S_2–L_2 fabrics (Fig. 4c). The relationships between the dip of S_2 and the plunge of corresponding lineations denote large geometrical variations. Wrenching on mainly gently (10–30°), but sometimes steeply dipping planes, is commonly accompanied by thrust-type relationships. Whilst the latter situation results in obvious oblique or nearly transverse cartographic L_2 distributions, the occurrence of thrust-type relations in steeply dipping (up to 80–90°) S_2 implies that, locally, important vertical movements accompanied wrenching. Shear-sense criteria in the areas of gently dipping foliations denote SSE-directed tectonic motions compatible with coeval sinistral wrenching recognized in the areas with steeply dipping S_2. These features characterize D_2 transpressional tectonism, deformation partitioning into parallel and oblique–transverse components leading the accommodation of shortening components through oblique and transverse tangential motions and vertical tectonism. D_1 and D_2 structures were occasionally recognized in the same outcrop (Fig. 4g). SSW-vergent inclined or recumbent folds bear N–S mineral and stretching lineations. They have been preserved in rock volumes with a shallow dipping anisotropy (the S_0+S_1 fabric; Fig. 4g). When this anisotropy becomes steeper, L_1 is reoriented to the trends of D_2 and, locally, new shallow plunging L_2 stretching lineations appear. The geometry of reorientation of L_1 to the trends of D_2 is presented in Figs. 4(e) & (f), as recognized at some outcrops with deformed L_1. N–S-trending and variably plunging L_1 with large pitch values are deformed by reorientation towards the N130–140E direction. A de-

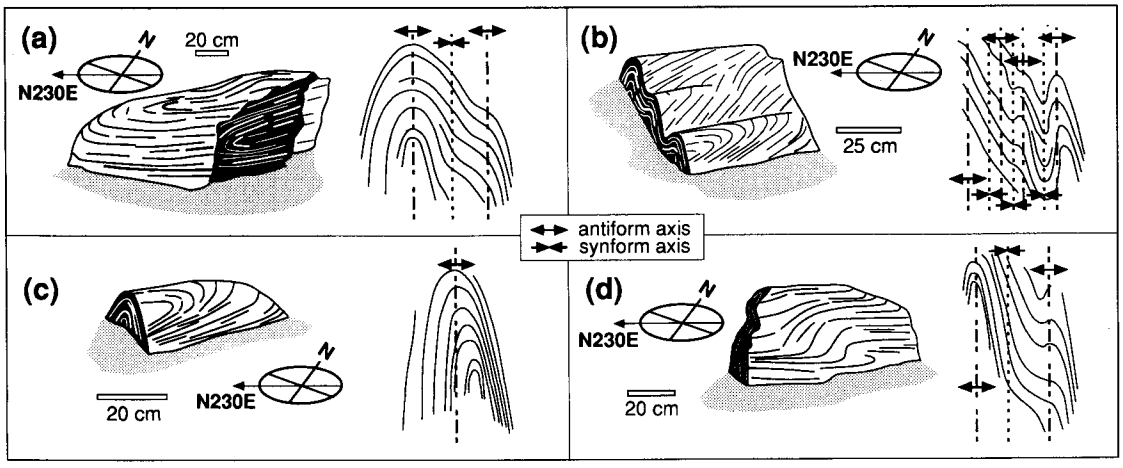

Fig. 6. (a)–(d) represent the four types of fold and lineation 'hairpin' morphologies cited in the text and the characteristics of L_1 geometrical distributions with respect to the axial trends of folds (antiform and synform axes differentiated) on the unrolled surfaces that contain the lineations.

crease in pitch values is then observed, with the higher the initial pitch angle, the higher the reorientation angle towards wrench-type S–L relationships (Fig. 4f). These features allow reinterpretation of orientation data collected systematically at some areas (Fig. 4d), in which clear differentiation of L_1 and L_2 is possible.

Whilst D_2 folds with axes parallel or variably oblique with respect to the L_2 are widespread in most areas northeast of the Atalaya window, in the Mina Afortunada dome (Fig. 2), some black quartzite layers contain L_1 structures that exhibit a particular and complex pattern of folding. Abalos (1990) has distinguished four fold types and the lineation deformational patterns shown in Fig. 6. The geometry of deformed lineations is characterized by a curvilinear arrangement on the unfolded foliation surfaces. The structural analysis of these structures establishes that: (1) the early lineations (L_1) were reoriented and/or transposed during a later (D_2) tectonic event; (2) heterogeneous simple shear was responsible for the generation of these structures; (3) heterogeneous shear exhibits maximum stretching in the NE–SW direction and associated top-to-the-southwest shear-sense criteria; (4) the mechanisms of D_2 folding were areally variable; and (5) S_1 and L_1 were SE-dipping and N–S-trending structures, respectively (Fig. 7).

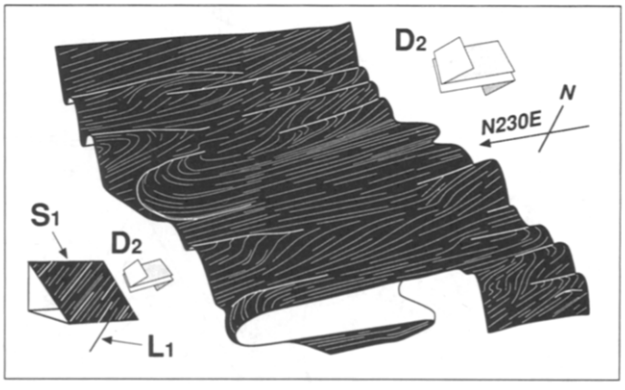

Fig. 7. Simplified tentative reconstruction of the geometry and orientation of the early structures (pre-Variscan S_1 and L_1) with respect to the trends of the Variscan superimposed deformation (D_2), and of the final stage of heterogeneous folding in a transpressive ductile shear zone.

MYLONITE FABRIC DEVELOPMENT IN THE DSB

Since a general idea of microstructures and shear-sense indicators preserved in different lithologic types was given above, the ongoing section will be concerned only with quartz petrostructural analysis. Quartz microstructures and fabrics have been studied with a universal stage in thin sections cut parallel to the XZ plane of finite strain frame ($X \geq Y \geq Z$; XY: plane of mylonitic foliation; X direction: stretching lineation). The grain size of dynamically recrystallized quartz new grains was used to calculate deviatoric stresses assuming that the general conditions for reliable geopiezometry are given (Twiss 1977). The geopiezometric calibrations of Mercier *et al.* (1977), Twiss (1977), White (1979) and Etheridge & Wilkie (1981) were used. Fabrics, microstructures and geopiezometric estimates exhibit rather different characteristics on either side of the Atalaya window.

Quartz microstructures

Southwest of the Atalaya window the size of dynamically recrystallized quartz grains average 90 μm in areas with mosaic textures in S-bands and 30 μm or less in the planes of shear. In the most deformed mylonitic gneisses quartz polycrystalline ribbons are made of equant or elongated grains (grain size $\approx$10–15 μm). Orientations of quartz sub-boundaries, deformation bands and lamellae become parallel to the direction of local mylonitic foliation in intensely deformed rocks. These textures have been experimentally obtained under geologically fast strain rates (Dell'Angelo & Tullis 1989).

In the Atalaya window quartz grains have a relatively small size (40–60 μm) and exhibit some dynamic recrystallization to subgrains and new grains. Some ribbons are deformed by sheath folds in which quartz shows sub-

boundaries and deformation lamellae defining a shape fabric oblique to the foliation. Samples without evidence of quartz plastic deformation occur often, as well as samples with flattened grains, which suggest a coaxial deformation history.

Quartz microstructures northeast of the Atalaya window reflect rather important variations. The grains with the largest sizes (80–100 μm) exhibit irregular bulged boundaries, undulous extinction, and are crossed by sub-boundaries at high angles to the foliation. Initially flattened quartz grains are transformed progressively into a mosaic of elongated grains of 40–70 μm in lower structural levels. In the Mina Afortunada area quartz grain size is reduced up to 20 μm and equigranular textures made of new grains form. D_1 microstructures in migmatites are mosaics of equant grains with triple junctions which obliterate earlier mosaic textures such as those described by Gapais & Barbarin (1986).

Quartz c-axis fabrics

In the area southwest of the Atalaya window extensive D_2 mylonitization results in the development of remarkable crystallographic fabrics (Fig. 8). The Ribera del Fresno gneiss exhibits markedly asymmetric fabrics defined by *c*-axis concentrations on *Y* (prism ⟨*a*⟩ slip) and between *Y* and *Z* (rhomb ⟨*a*⟩ slip) (Fig. 8c). Interesting relations are observed between shape–elongation of quartz grains and the respective *c*-axis orientation. Fabric relations such as these have been described before by Knipe & Law (1987) and Krohe (1990), who interpret them as the result of recrystallization-driven fabric development. Accordingly, Wenk *et al.* (1989) point out that such fabric relationships result from recrystallization processes favouring nucleation in the most strongly deformed grains, which are those favourably oriented for slip and allowed to deform at a faster rate. In the gneissic units surrounding the Ribera del Fresno gneiss no fabric memory related to D_1 was preserved. D_2 quartz *c*-axis fabrics correspond to single girdles uniformly oblique to *XY* and defined by *c*-axis maxima on *Y* and between *Y* and *Z* (Figs. 8a & b). In most cases these fabrics exhibit the characteristics ascribed to fabric development under simple shear. However, some asymmetric kinked single girdles (controlled by the two *c*-axis orientations where double rhomb ⟨*a*⟩ slip is possible; Fig. 8b) might characterize general heterogeneous deformation diverging slightly from the simple shear model (Mancktelow 1987).

In the Atalaya window quartz *c*-axis fabrics are often weak and lack a clear relation with respect to the structural and kinematic framework (Fig. 9b). In spite of these finds, there may usually be found microstructural criteria denoting superposition of low-grade D_1 and D_2 deformations and local, ductile D_2 shearing.

Northeast of the Atalaya window quartz *c*-axis fabrics record the superposition of D_1 and D_2. In the migmatites of the Mina Afortunada dome, *c*-axis maxima parallel to the megascopic stretching lineation occur (Fig. 9a). These maxima are interpreted as indicating prism ⟨*c*⟩ slip and plastic deformation under temperatures at least of the upper amphibolite facies (Garbutt & Teyssier 1991) or—most likely—near the granite solidus (Mainprice *et al.* 1986). In the domains subjected to D_2 mylonitization

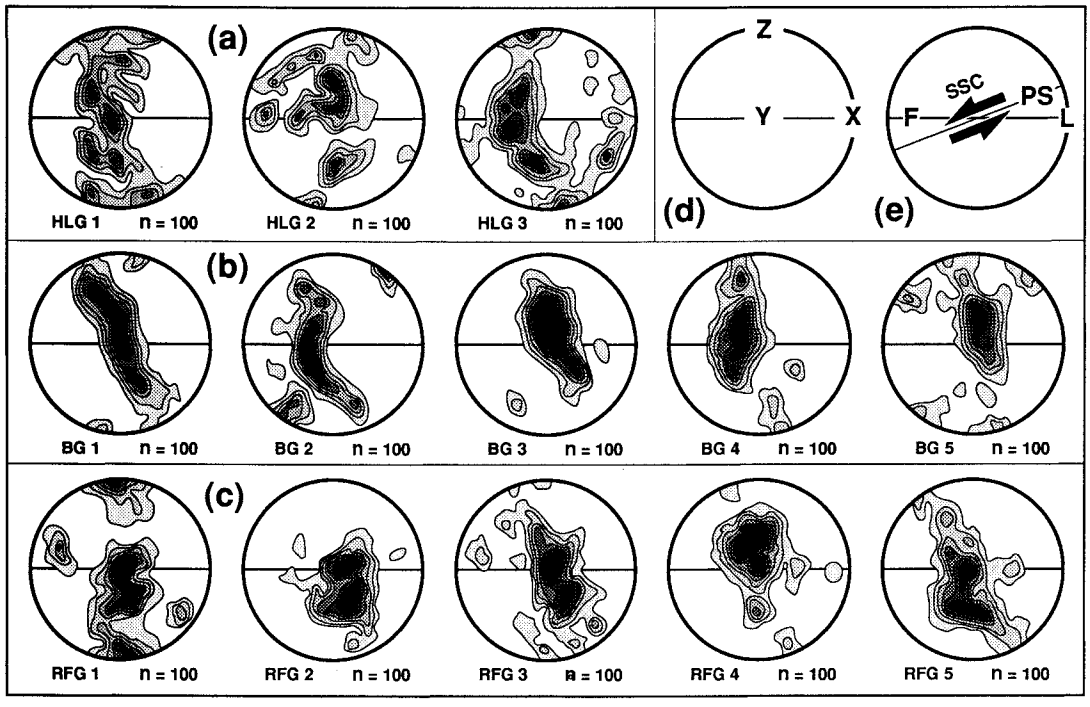

Fig. 8. Quartz *c*-axis fabric diagrams for gneisses from the area southwest of the Atalaya window ductilely deformed during D_2 under moderate temperatures (500–550°C). (a) Higuera de Llerena mylonite gneiss. (b) Biotite- and muscovite-rich gneisses from the blastomylonitic migmatitic unit. (c) *S–C* orthogneisses (RFG1, RFG2 and RFG3), aplites (RFG4) and greisen (RFG5) from the Ribera del Fresno window. (d) Structural *XYZ* reference axes. (e) Alternative reference framework in *XZ* section with F (mylonitic foliation), L (stretching lineation), PS (plane of shearing) and SSC (shear-sense criteria). Contour intervals 1%.

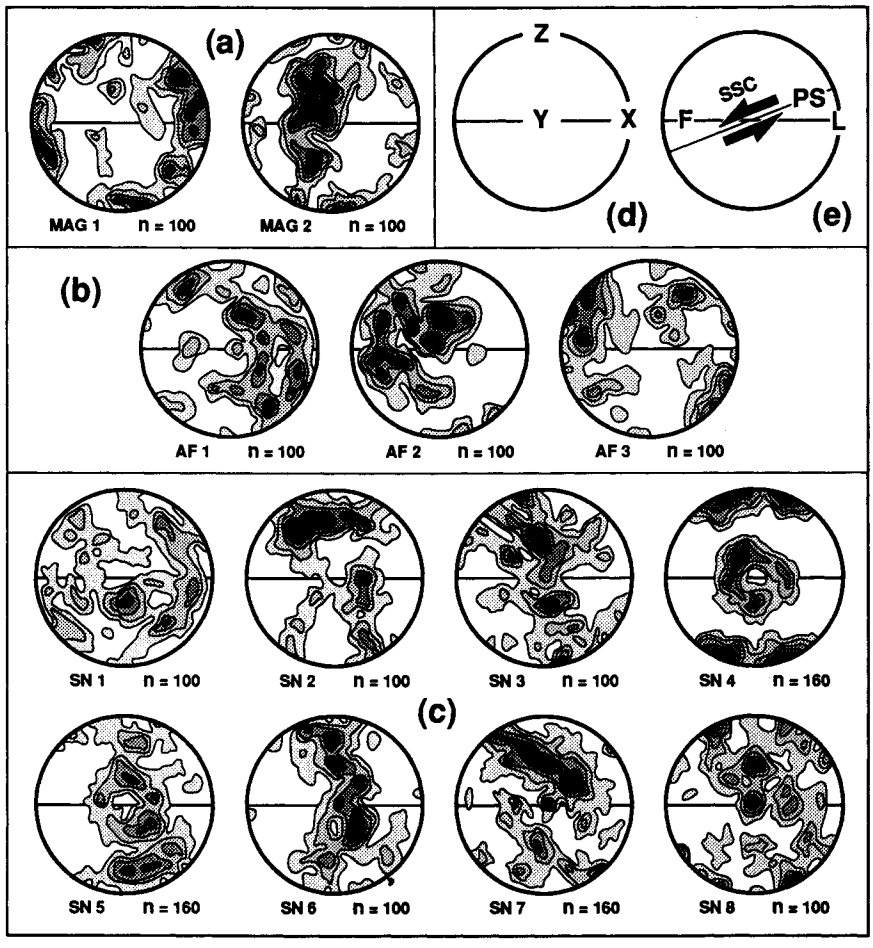

Fig. 9. Quartz *c*-axis fabric diagrams for: (a) migmatites from the base of the Serie Negra (Mina Afortunada gneiss dome); (b) low-grade schists from the Atalaya window; and (c) black quartzite layers interbedded in the Serie Negra. (d) Structural *XYZ* reference axes. (e) Alternative reference framework as in Fig. 8(e). Contour intervals 1%.

quartz *c*-axis fabrics define single girdles at high angles with respect to the *XY* plane delineated by *c*-axis maxima situated on the *Y* direction and close to *Z*. The *c*-axis fabrics in black quartzites from the Serie Negra exhibit a regular variation from upper to the lowermost structural levels. Fabrics in the uppermost structural levels are weak and asymmetric with respect to the *XYZ* frame (e.g. SN1 in Fig. 9c). Weak *c*-axis maxima form small girdles along small circles centred on *Z* and are also located between *Z* and *Y* (e.g. SN2, SN4 and SN5 in Fig. 9c). In lower structural levels *c*-axis maxima on *Y* appear and the angle between the girdle and the *XY* plane decreases (e.g. SN3 and SN8 in Fig. 9c). In lowermost structural levels application of the basal plane shear-sense criteria may give kinematic results in contradiction with shear-sense determinations using microstructures, as previously recognized by Carreras *et al.* (1977). The black quartzites sometimes exhibit D_2 sheath folds with their hinges parallel to the mineral and stretching lineations (Fig. 10). When the *c*-axis fabrics measured in the two fold limbs of a representative specimen are similar (Fig. 10a), this fact perhaps indicates that the axial plane of the fold acted as an active flow plane during shearing and that a new fabric pattern related to this flow plane developed. Both limbs of the fold would indicate therefore the same shear sense (Stünitz 1991). However, if the fabric pattern had been passively rotated, the normal and inverted limbs would display opposite shear senses (Fig. 10b).

Mechanisms and temperature conditions of D_1 *and* D_2

Quartz microstructures and the *c*-axis patterns presented above indicate that D_2 took place under temperature conditions characteristic of low- and medium-grade metamorphism.

Southwest of the Atalaya window prism ⟨*a*⟩ slip acquires increasing importance and enables accommodation of large strain under dominant simple shear. Accommodation of coaxial strains results in the kinking of *c*-axis girdles. However, strong *c*-axis maxima on the *Y*-axis are prevalent as a result of dynamic recrystallization processes. The temperatures prevailing during D_2 in this area range between 400 and 550°C.

Deformation within the Atalaya window and northeast of this structure are controlled mainly by basal and rhomb ⟨*a*⟩ slip. Qualitative D_2 strain path assessment is possible from the general external asymmetry of quartz *c*-axis fabrics, which can be interpreted as indicating prevalent non-coaxial deformations. The occurrence of *c*-axis girdles along small circles centred on *Z* is interpreted as due to coaxial deformation coeval with or following rotational strain components (Schmid &

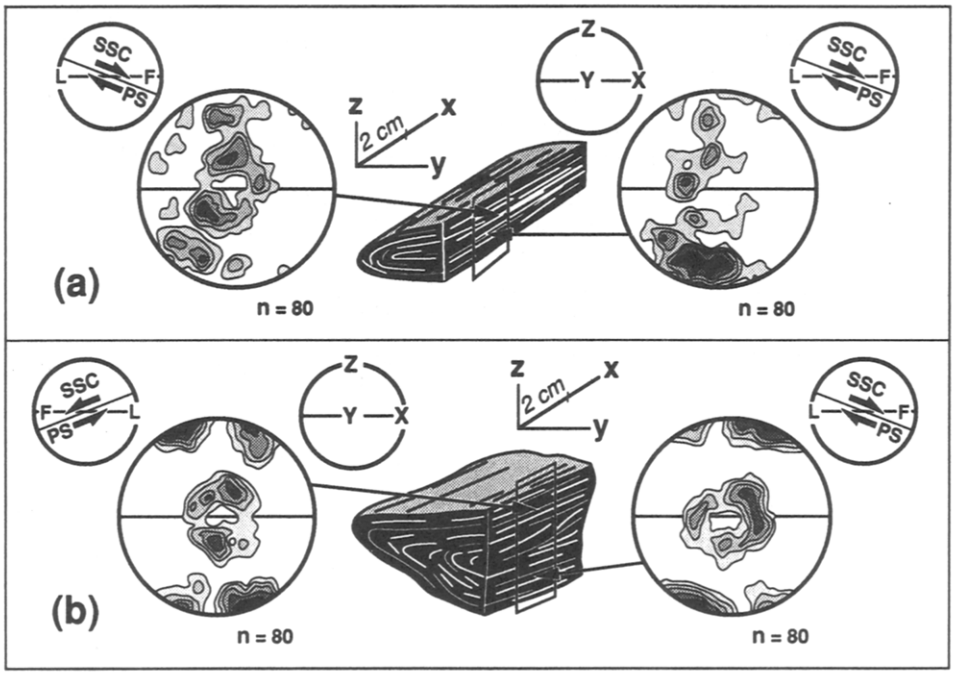

Fig. 10. Structural sketches of folded black quartzite hand specimens and equal-area lower-hemisphere quartz *c*-axis orientation diagrams for the two limbs of isoclinal folds with axes parallel with the stretching lineation. Contour intervals 1.25%. *XYZ* structural references are given. (a) Shear-sense criteria (SSC) deduced from the relative positions of megascopic foliation (F), stretching lineation (L) and the deduced plane of shearing (PS) for the two limbs coincide, and support fold mechanisms with prevailing simple shear. (b) Shear-sense criteria deduced for the two limbs are converse, and support fold mechanisms in which the folding of a previously deformed quartzite layer is prevalent.

Casey 1986). The temperatures prevailing during D_2 in these areas range between 300 and 400°C, temperatures of 400–550°C being attained although locally (Mina Afortunada dome). D_1 in migmatites of the Serie Negra occurred under temperatures of 600–650°C.

Geopiezometry–geospeedometry

Southwest of the Atalaya window D_2 textures in blastomylonitic gneisses reflect deformation under low deviatoric stresses (20–25 MPa; Fig. 11). Strain gradients associated with the formation of shear surfaces in mylonites are accompanied by harmonious deviatoric stress gradients varying from 40–50 to 80–120 MPa. Deviatoric stresses calculated for recrystallization in D_2 ultramylonite bands are occasionally very high (up to 150 MPa). The concurrent strain rates vary between 10^{-13} and 10^{-15} s^{-1} for blastomylonites and 10^{-11}–10^{-12} s^{-1} for ultramylonites. Since the temperature of quartz plastic deformation was not very different in both, the differences in strain rates are probably due to stress concentration in discrete anisotropy surfaces.

Northeast of the Atalaya window geopiezometric estimates indicate the presence of a gradient for D_2 deviatoric stresses at the map scale. These range between background values of 30 MPa 1.5 km above the basal thrust of the Serie Negra onto the para-autochthon and 90–100 MPa near the thrust. Stress gradients such as those reported above for formation of mylonite gneisses occurred during D_2 in the Mina Afortunada dome. The strain rates calculated for these rocks span between 10^{-14} s^{-1} in upper parts of the Serie Negra and 10^{-12} s^{-1} at its base.

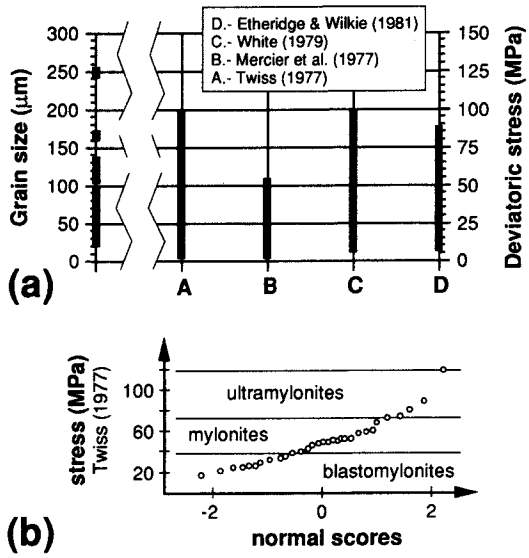

Fig. 11. (a) Size of dynamically recrystallized quartz new grains (in μm) vs deviatoric stresses (in MPa) for ductile tectonites of the DSB. (b) Normal probability plot showing the distributions or ranges of variation of the deviatoric stresses (MPa) calculated through Twiss's (1977) geopiezometer for the empirically observed development of tectonites in the DSB.

The Azuaga and Hornachos master faults bounding the DSB are associated with bands of fault rocks (ultramylonite–cataclasite–fault breccias) locally 200–300 m thick. Microstructures often indicate cyclic ductile quartz deformation complexly overprinted by brittle deformations and microfailure (the converse is also observed). In the Azuaga fault the grain size of dynamically recrystallized quartz grains is in the range 20–35 μm, and the corresponding deviatoric stresses vary be-

tween 60 and 100 MPa. In the Hornachos fault quartz grain size is often slightly higher (30–40 μm) and the respective deviatoric stresses range 50–70 MPa. According to Blenkinsop & Drury (1988) these stress values are of the same magnitude as the stress levels characteristic of fault zones above the frictional–quasi-plastic boundary. The strain rates calculated for the Azuaga and Hornachos faults (in the range 10^{-12}–10^{-13} s^{-1}) indicate that the relative movements between the blocks they bound (accommodated sporadically and cyclically) took place at moderate velocities of the order of a few cm yr^{-1}, similar to those depicted for current active faults (Pfiffner & Ramsay 1982).

DISCUSSION

Tectonic–kinematic model for the Cadomian orogenic wedge complex

High-pressure–high-grade M_1 metamorphism in the gneissic units of the DSB show microstructural synkinematic relationships with respect to D_1. The kinematic analysis of D_1 structures indicates a southwards emplacement direction related to the ductile deformation of these metamorphic allochthonous units. D_1 structures in the para-autochthonous unit and in the uppermost allochthonous slices are consistently verging southwards.

The *P–T* paths undergone by the high-grade gneissic slices and the *P–T* conditions recorded (Fig. 12) support a scheme of 'inverted metamorphism' interpreted in relation with crustal thickening processes (Abalos *et al.* 1991a). The areal distribution of late Precambrian synorogenic sequences, the variation of K_2O contents in calc-alkaline late Precambrian magmatic rocks across the DSB and the areas related to the southwest, and the disposition of the paired high-pressure Badajoz–Córdoba DSB and low-pressure Monesterio metamorphic belt situated to the south (Quesada *et al.* 1990, Eguíluz & Abalos 1992) suggest that the most likely geodynamic scenario for the Cadomian DSB was an Andean-type continental margin with a southward-dipping Benioff zone. As such, D_1 structures described in this study should be related to the late episodes of Cadomian tectonothermal evolution. Since the occurrence of early (subduction-related) Cadomian structures was not clearly evident, recognition of intra-late Precambrian unconformities in the BCSZ led Quesada (1990) to suggest two major Cadomian tectonic events. Their first could be related to subduction processes in a southward-dipping Benioff zone situated northeast of the DSB, and their second would correspond to D_1 described here. Given the 30–60° obliquity between L_1 stretching lineations and the trends of S_1 and D_1 tectonic contacts, an accretionary complex in a transpressional continental margin is proposed here to explain the Cadomian geodynamic evolution of the DSB.

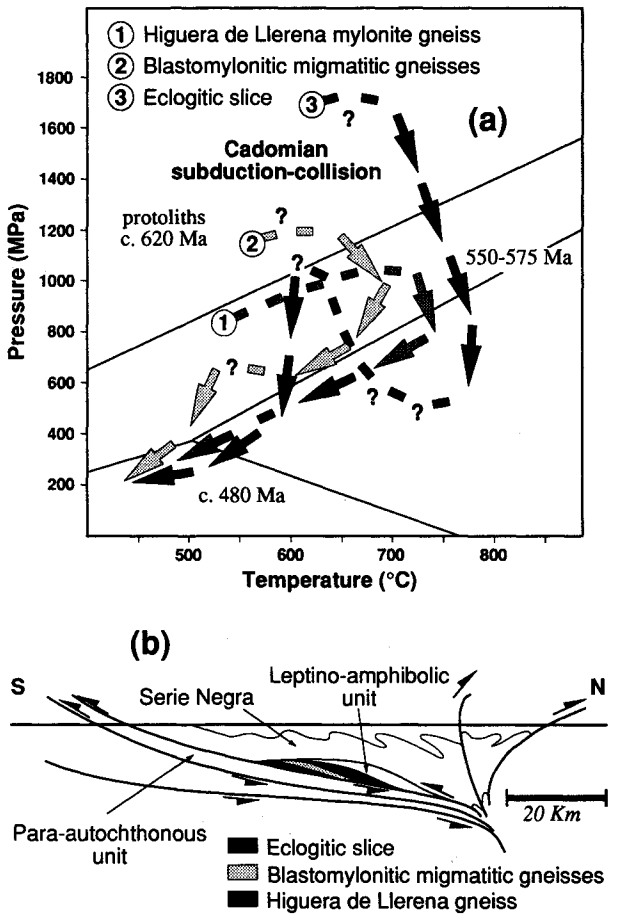

Fig. 12. (a) *P–T* paths for the Cadomian tectonothermal evolution of high-grade and high-pressure rocks of the DSB. (b) Tentative reconstruction of the Cadomian subduction–accretion wedge complex of SW Iberia.

Tectonic–kinematic model for the Variscan intracontinental shear zone

As it was highlighted in previous sections, deformation mechanisms, strain magnitude, deformation partitioning and reorientation–transposition of pre-Variscan structures, were strongly areal-dependent processes. At the scale of the BCSZ, large strike-slip faults bound different crustal blocks. Whilst transpressive deformations gave rise in the Obejo–Valsequillo domain (Fig. 1b) to NE-vergent steep thrusts, inclined folds with associated axial plane slaty cleavage, and NW–SE sinistral strike-slip faults, the DSB conforms to a Variscan fault-bounded narrow zone of sinistral ductile wrenching separating two crustal domains with opposite structural vergences (Fig. 13).

The DSB is itself internally partitioned by the Atalaya window into three belts with different characteristics. This structure constitutes a zone of heterogeneous deformation sharing some common features with the blocks it bounds. Northeast of the Atalaya window reorientation of early structures was dominant during Variscan deformation, ductile deformation being observed locally (Fig. 14c). Coaxial Variscan deformations coeval with or following rotational strain components are mainly observed in this epizonal band. On the other hand, in the area southwest of the Atalaya window

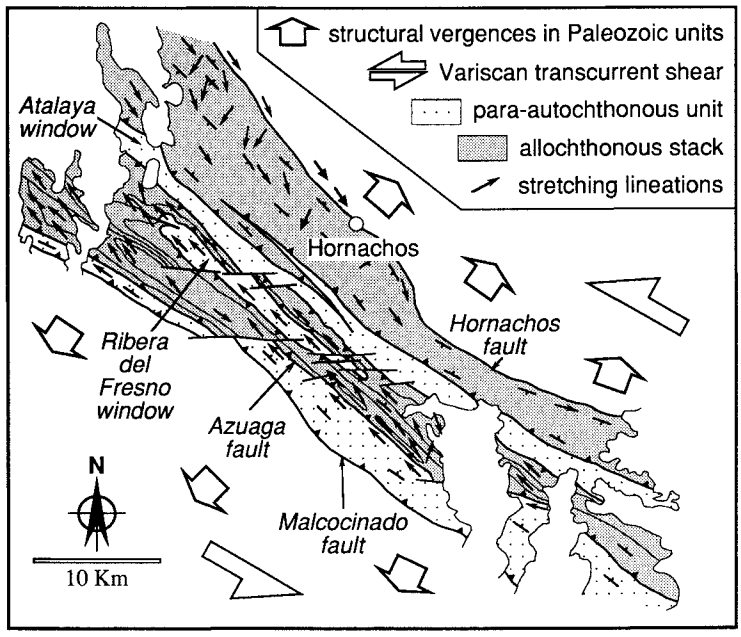

Fig. 13. Structural map showing the kinematics of D_2 stretching lineations (arrows) and the vergence of Variscan structures in the Palaeozoic rocks situated at both sides of the DSB: NE-vergent structures northeast of the Hornachos fault (Obejo–Valsequillo domain), and SW-vergent structures southwest of the Azuaga and Malcocinado faults.

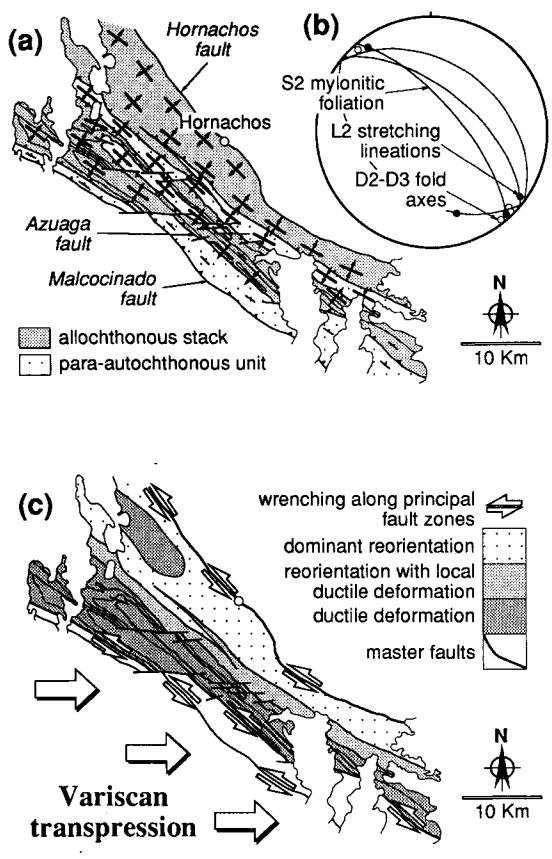

Fig. 14. (a) Structural map showing the trends of Variscan folds deforming the stack of late Precambrian medium- and high-grade rocks of the DSB. (b) Equal-area lower-hemisphere stereoplot depicting the relationships between orientation of D_2–D_3 fold axes, L_2 stretching lineations and S_2 mylonic foliations. Orientation data plotted were obtained from axial Bingham statistical analysis of 838 and 820 linear data concerning S_2 and L_2, respectively. (c) Highly schematic representation of the areal distribution of prevalent deformation styles in the DSB and the kinematics of master faults in relation with a regional transpressive Variscan stress field.

pervasive ductile deformations almost entirely erased previous structures. Non-coaxial Variscan deformation or strain paths were dominant in this mesozonal band.

Ductile and brittle–ductile deformation of the pre-Variscan basement gave rise in the DSB to the folding of Cadomian foliations and tectonic or lithostratigraphic contacts. D_2–D_3 folds and tectonic windows of the basal thrust of the allochthonous stack were formed with their axes parallel to the trend of L_2 stretching lineations and D_3 master strike-slip faults (Figs. 14a & b). Ductile deformations exhibit an increase in intensity with depth and towards the southwest, as revealed by positive strain gradients in the Mina Afortunada area and by the augmentation of the temperature of deformation towards the Azuaga fault zone (Fig. 14c). The latter fault exhibits several features supporting the overprinting of ductile structures by brittle–ductile and brittle deformations during a cyclic but continuous process, at decreasing temperatures. These variations were perhaps induced by allied stress gradients (up to 100 MPa) and point to the Azuaga fault zone as a major constraint to the Variscan evolution of the DSB.

Northeast of the Atalaya window L_2 lineations are often oblique or transverse with respect to the dominant strike of D_2 foliations and lithologic contacts (Fig. 13). Shear-sense criteria denote SSE-directed tectonic motions compatible with sinistral shearing in the band southwest of the Atalaya window and with general Variscan sinistral wrenching in the BCSZ. This kinematic scheme might indicate that tangential (SSE-directed) and wrench (left-lateral) tectonic components were coeval. Accommodation of three-dimensional bulk transpressive strain in the DSB probably took place by means of deformation partitioning into parallel and oblique–transverse components. Pre-existing gently dipping bed-

ding, foliated medium, or lithologic–tectonic contacts, could drive this process and constrain accommodation of shortening components through internal strain and transverse tangential components. Such gently dipping anisotropy should play the same kinematic role in wrench systems as do lateral ramps in dip-slip systems.

Direct estimation of Variscan tectonic displacements in the BCSZ and the DSB is speculative, given the absence of passive markers at both sides of these structures. Application of Peacock & Sanderson's (1991) algorithm for fault length vs displacement relationships to the Hornachos and Azuaga faults results in sinistral tectonic displacements of 45 and 55 km, respectively. However, in principle these figures do not account for their tectonic translations during the early ductile and brittle–ductile history.

Early attempts to quantify the magnitude of sinistral tectonic displacements and the state of strain of mylonites from the DSB by Burg *et al.* (1981) resulted in a figure of 72 km sinistral displacement. The quantification of the state of strain of gneisses from the DSB by Abalos (1990), using feldspar centres as markers, enabled determination of contrasting strain paths in the bands northeast and southwest of the Atalaya window and recognition of large heterogeneities at the scale of the gneiss massifs studied (Fig. 15). Finite strain ellipsoids and the respective strain paths from the Mina Afortunada gneiss plot in the field of apparent flattening. This result, together with the occurrence of rolling structures, enable estimation of minimum shear strain of $\gamma = 5$–8. Southwest of the Atalaya window finite strain ellipsoids from the Ribera del Fresno gneiss and the respective strain paths plot in the field of apparent constriction. Shear strain values between 0.58 and 1.73 were calculated. Composition of the magnitude of tectonic displacements in the DSB on the basis of the previous determinations results in a figure of 25 km sinistral wrench.

An alternative evaluation of Variscan tectonic displacements on the basis of the strain rates, described in the geopiezometry section, considers such displacements as the sum of various components. Deformation under temperatures of 450–550°C and strain rates of 10^{-14}–10^{-15} s^{-1} was probably a long-lived event, since cooling from ≈500 to ≈350°C took about 30 Ma (Dallmeyer & Quesada 1989). This process could represent transcurrent tectonic displacements of the order of some tens of km accommodated by mylonites–blastomylonites. Ductile deformation in the ultramylonite bands took place under comparable temperatures and very fast strain rates of 10^{-11}–10^{-13} s^{-1}. These strain rates are comparable to tectonic displacements of a few cm yr^{-1} and imply that tectonic motions of several tens of km could occur in 1 Ma or less.

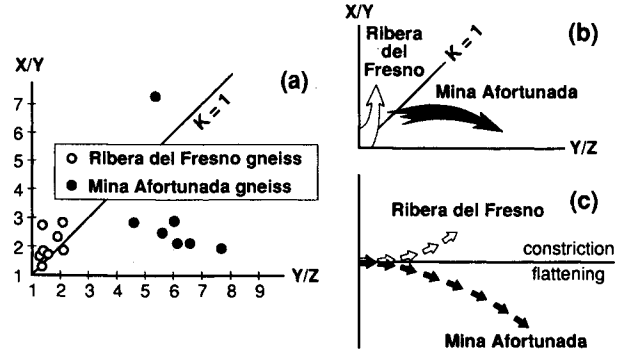

Fig. 15. (a) Flinn's diagram showing finite strain ellipsoids obtained through the Fry's technique in gneisses from the Mina Afortunada dome and Ribera del Fresno window. (b) Respective strain paths in the fields of apparent flattening (Mina Afortunada gneiss dome) and constriction (Ribera del Fresno gneiss; Fig. 2). (c) Contrasted evolution of deformation vs time towards the fields of flattening and constriction.

In summary, sinistral transcurrent displacements in the DSB may be considered as the sum of: (1) tectonic displacements of some tens of km accommodated by medium-grade tectonics; (2) displacements of several tens to a few hundreds of km accommodated by ultramylonite corridors; and (3) displacements of at least 50–60 km accommodated by each of the Azuaga and Hornachos fault zones. These components could easily result in transcurrent tectonic displacements of 300–400 km between the blocks situated at both edges of the DSB during the 370–320 Ma time span.

Implications for the tectonic evolution of the Ibero-Armorican arc

The close resemblance existing between the geology of the Armorican and Iberian Massifs traditionally led many authors to consider that a major structural feature originally existed, the Ibero-Armorican arc, correlating these massifs across the Bay of Biscay (Le Fort 1983). It has largely been suggested that formation of the arc took place along the Middle–Upper Palaeozoic in the course of the Variscan orogeny. The occurrence of both transverse and oblique stretching lineations associated with major thrust zones has been recognized by Burg *et al.* (1987) in the northern branch of the Ibero-Armorican arc. These authors interpret such structural features as the result of collisional events driven by a transform zone at a high angle to a convergence–subduction zone (the 'corner effect' tectonic model).

The BCSZ in this and comparable kinematic models is regarded as a Variscan suture evolving into an intracontinental shear zone. However, the poly-orogenic evolution of the BCSZ shown in this study tends to contradict such a statement. Variscan strike-slip tectonism is of course a major feature of both branches of the Ibero-Armorican arc. In the southern Iberian Massif this tectonism was constrained by intracontinental wrenching in the BCSZ and oblique underthrusting of the South Portuguese domain beneath the Ossa–Morena along the Southern Iberian Shear Zone (Crespo-Blanc & Orozco 1988, Abalos *et al.* 1991b), which should be regarded as the true Variscan suture zone of SW Iberia.

Variscan transpressive events in the BCSZ and the DSB may be easily related to the overall flower structure exhibited by major structures (Abalos 1990) and to coeval tangential tectonism in neighbouring structural

domains, namely: (1) SW-directed thrust and fold-nappe emplacement (inverted limbs up to 20 km in length) in the central and southern Ossa–Morena (Vauchez 1975, Crespo-Blanc & Orozco 1988, Eguíluz 1988); and (2) NE-vergent folding and thrust emplacement northeast of the BCSZ.

The magnitude of sinistral transcurrent displacements accommodated by the DSB and the BCSZ during the Variscan is comparable to the magnitude of the late Palaeozoic tangential thrust associated with high-grade nappe-complexes with mafic–ultramafic suites of NW Iberia (a few hundreds of km; Matte 1991).

The reconstruction of the circum-Atlantic Cadomian orogen

Pre-Variscan plate reconstructions of the western European Hercynides should bear in mind that the Ossa–Morena was probably located a few hundreds of km to the west of its actual position, but still in connection with the Central Iberian Zone, during the early and Middle Palaeozoic.

Capdevila & Mougenot (1988) suggested that the Ossa–Morena represents the eastern margin of Avalonia later involved in the Variscan orogeny. The Variscan evolution of the DSB constrained the tectonic evolution of the Ossa–Morena area situated to the south by large sinistral shearing episodes. In Fig. 16(a) the magnitude of the tectonic displacements accommodated by the BCSZ is used to restore the Ossa–Morena to its original position before the late Palaeozoic shearing. With a *ca* 400 km displacement to the northwest and a clockwise rotation of about 45°, the Ossa–Morena block fills the void existing between the borderline of the Grand Banks of Newfoundland and the western Iberian continental margin in pre-Mesozoic plate assemblies. Moreover, Cadomian structures in the Ossa–Morena parallel the structural trends found in the Avalon peninsula and its continuation in Atlantic Canada (Galdeano *et al.* 1990).

The DSB and the low pressure–high temperature Monesterio metamorphic terrane (Eguíluz & Abalos 1992) represent a pair of metamorphic belts situated in the oceanic and continental sides, respectively, of an Andean continental margin. Geometrical relationships of actual structures (related to Cadomian terrane accretion) support the underthrusting of terranes situated to the south beneath northern terranes within an orogenic wedge complex.

The Cadomian geodynamic evolution of the Ossa–Morena shares several common features (comparable chronology of deformation, metamorphism and calc-alkaline magmatism; similar geodynamic context in an Andean-type continental margin; coeval subduction and collisional events, etc.) with those of the neighbouring areas, i.e. the North Armorican Massif, Anglesey, Avalonia and the west African/southeast North American late Precambrian orogens. In Fig. 16(b) available kinematic and structural data for these areas are presented and used to reconstruct the late Precambrian orogen of the North Atlantic.

A change in the tectonic polarity from subduction to arc–continent collision as reported above for the Ossa–

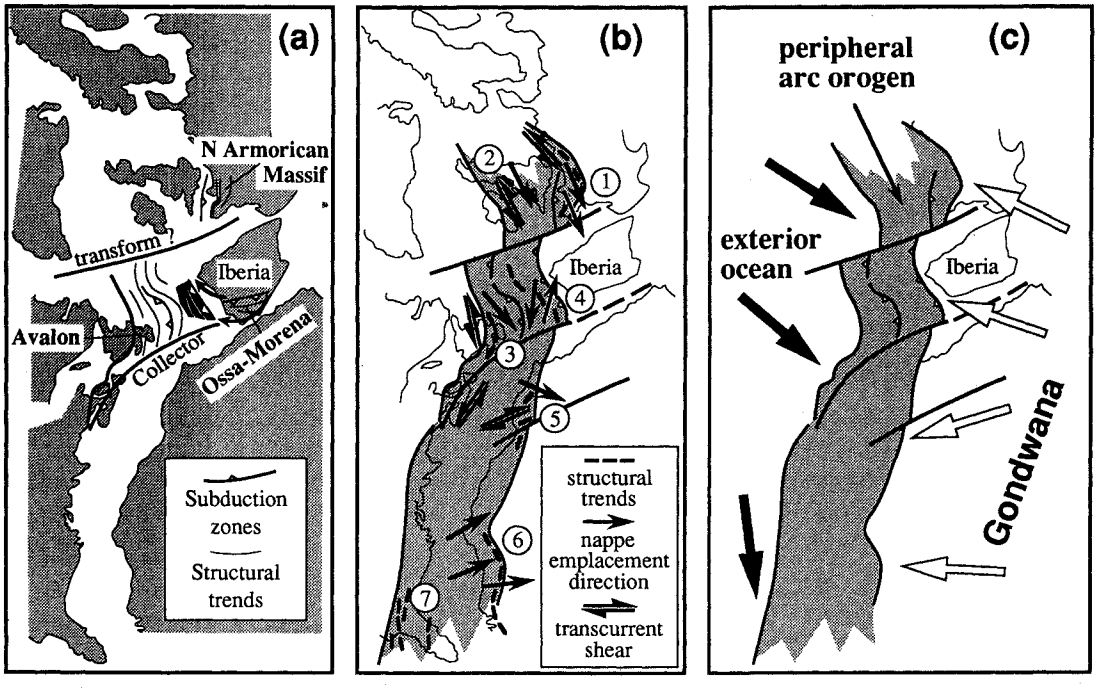

Fig. 16. Reconstruction of the Cadomian–Avalonian–Panafrican orogen of the North circum-Atlantic borderlands. (a) Restoration of the Ossa–Morena to its position prior to the late Palaeozoic (see text for further details). (b) Kinematic and structural data for different areas of the Cadomian–Avalonian–Panafrican orogen collected from: (1) Balé & Brun (1989), Strachan & Roach (1990), and Treloar & Strachan (1990); (2) Murphy (1990); (3) Gibbons (1990) and Nance (1990); (4) Quesada *et al.* (1990), Eguíluz & Abalos (1992), and this study; (5) Ighid *et al.* (1989); (6) Dallmeyer & Lecorche (1990) and Villeneuve *et al.* (1990); (7) Dallmeyer (1989). (c) Reconstruction of the late Precambrian transpressive margin and main tectonic displacement vectors related to oblique plate convergence.

Morena has been also recognized in the Northern Armorican Massif in the 590–540 Ma time span (Rabu *et al.* 1990). Although different kinematic interpretations of Cadomian structures exist (Balé & Brun 1989, Strachan & Roach 1990, Treloar & Strachan 1990) prevalent NE–SW nappe emplacement or sinistral wrenching are often interpreted as reflecting oblique subduction–collision. In the Anglesey–Ireland area WSW sinistral transpression was recognized by Murphy (1990). In the Avalon zone of eastern Canada only subduction of late Precambrian crust and transcurrent terrane dispersal by oblique sinistral plate convergence have been documented in this period (latest Precambrian–earliest Cambrian, 550–540 Ma; Gibbons 1990, Nance 1990). Nappe emplacement and main kinematic directions for the structures preserved in the Panafrican II West African orogens and the southeastern United States (Florida Peninsula), adjacent in pre-Mesozoic plate reconstructions, are poorly constrained. However, southeast and east nappe emplacement directions have been proposed by Dallmeyer (1989), Ighid *et al.* (1989), Dallmeyer & Lecorche (1990) and Villeneuve *et al.* (1990). These directions are consistent with NNW–SSE compression (resulting in NE–SW-striking structures) oblique with respect to the general N–S trend of the late Precambrian orogen in this area.

Although in detail the kinematic data presented are heterogeneous, they are consistent with a general scheme of oblique plate convergence and strike-slip orogenesis, sinistral wrench components being dominant at the scale of the orogen during the stages of arc–continent collision. Late Precambrian–early Cambrian oblique convergence between Gondwana and an exterior ocean (Murphy & Nance 1989, 1991) can congruently explain the decomposition of convergence tectonic vectors into transverse, oblique and parallel movement zones at different areas during the subsequent tectonic evolution (Fig. 16c).

CONCLUSIONS

It is concluded that polyphase deformation and metamorphism in the Badajoz–Córdoba DSB are the result of a poly-orogenic evolution including late Precambrian accretion of mid- and lower-crust tectonic slices in an orogenic wedge complex, and the development of an intracontinental ductile shear zone during the Variscan orogeny. The intracontinental transcurrent displacements accommodated by the DSB and the BCSZ during the late Palaeozoic imply that in pre-Variscan plate reconstructions of western Europe the Ossa–Morena was probably located a few hundred km to the west of its actual position, but still in connection with the Central Iberian Zone of western Iberia. Kinematics of late Precambrian structures in the DSB and the related Cadomian–Avalonian–Panafrican areas of the circum-Atlantic region are consistent with a scenario of oblique convergence in a transpressional margin. All these processes denote the poly-orogenic nature of the DSB and exemplify large-scale tectonic displacements along strike in transpressive orogens of different age.

Acknowledgements—A review by Dr R. A. Strachan (Oxford Polytechnic) and editorial comments from Dr S. H. Treagus greatly helped to improve the organization and presentation of this paper and are much appreciated. Financial support for this paper was provided by the Univ. del País Vasco (projects E097/90 and E135/91).

REFERENCES

Abalos, B. 1990. Cinemática y mecanismos de la deformación en régimen de transpresión. Evolución estructural y metamórfica de la zona de cizalla dúctil de Badajoz–Córdoba. Unpublished thesis. Univ. País Vasco.

Abalos, B., Eguíluz, L. & Gil Ibarguchi J. I. 1991a. Cadomian subduction/collision and Variscan transpression of the Badajoz–Córdoba shear belt (SW Spain). *Tectonophysics* **199**, 51–72.

Abalos, B., Gil Ibarguchi, I. & Eguíluz, L. 1991b. Structural and metamorphic evolution of the Almadén de la Plata Core (Seville, Spain) in relation to syn-metamorphic shear between the Ossa–Morena and South-Portuguese Zones of the Iberian Variscan Fold Belt. *Tectonophysics* **191**, 365–387.

Apalategui, O. & Pérez-Llorente, F. 1983. Nuevos datos en el borde meridional de la Zona Centro-Ibérica. El Dominio Obejo-Valsequillo-Puebla de la Reina. *Stvd. Geol. Salmanticensia* **18**, 193–200.

Balé, P. & Brun. J.-P. 1989. Late Precambrian thrust and wrench zones in northern Brittany (France). *J. Struct. Geol.* **11**, 391–405.

Bell, T. H. & Rubenach, M. J. 1980. Crenulation cleavage development—evidence for progressive bulk inhomogeneous shortening from millipede microstructures in the Robertson River metamorphics. *Tectonophysics* **68**, T9-T15.

Bladier, V. 1974. Structure et Pétrologie de la Bande Blastomylonitique de Badajoz–Córdoba (Chaine Herynienne Sud-Ibérique á l'ouest d'Azuaga, Espagne). Les roches cataclastiques–classification–interpretation. Unpublished thése 3éme Cycle, Univ. Montpellier.

Blatrix, P. & Burg, J.-P. 1981. $^{40}Ar/^{39}Ar$ Dates from Sierra Morena (Southern Spain). Variscan metamorphism and Cadomian orogeny. *Neues Jb. Miner. Mh.* **10**, 470–478.

Blenkinsop, T. G. & Drury, M. R. 1988. Stress estimates and fault history from quartz microstructures. *J. Struct. Geol.* **10**, 673–684.

Bouchez, J.-L., Lister, G. S. & Nicolas, A. 1983. Fabric asymmetry and shear sense in movement zones. *Geol. Rdsch.* **72**, 401–419.

Buck, W. R. & Tocksöz, H. N. 1983. Thermal effects of continental collision; thickening a variable viscosity lithosphere. *Tectonophysics* **100**, 53–69.

Burg, J.-P., Balé, P., Brun, J.-P. & Girardeau, J. 1987. Stretching lineations and transport direction in the Ibero-Armorican Arc during the Siluro-Devonian collision. *Geodinamica Acta* **1**, 71–81.

Burg. J.-P., Iglesias, M., Laurent, Ph., Matte, Ph & Ribeiro, A. 1981. Variscan intracontinental deformation: the Coimbra-Córdoba Shear Zone (SW Iberian Peninsula). *Tectonophysics* **78**, 15–42.

Capdevila, R. & Mougenot, D. 1988. *Pre-Mesozoic Basement of the Western Iberian Continental Margin and its Place in the Variscan Belt* (edited by Boillot, G., Winterer, E. J., *et al.*). *Proc. ODP, Sci. Results* **103**, 3–12.

Carreras, J., Estrada, A. & White, S. 1977. The effects of folding on the *c*-axis fabrics of a quartz mylonite. *Tectonophysics* **39**, 3–24.

Crespo-Blanc, A. & Orozco, M. 1988. The Southern Iberian Shear Zone: a major boundary in the Hercynian folded belt. *Tectonophysics* **148**, 221–227.

Dallmeyer, R. D. 1989. Contrasting accreted terranes in the southern Appalachian orogen and Atlantic-Gulf Coastal Plains and their correlations with West African sequences. In: *Terranes in the Circum-Atlantic Paleozoic Orogens* (edited by Dallmeyer, R. D.). *Spec. Pap. geol. Soc. Am.* **230**, 247–267.

Dallmeyer, R. D. & Lecorche, J. P. 1990. $^{40}Ar/^{39}Ar$ polyorogenic mineral age record in the northern Mauritanide orogen, west Africa. In: *Terranes in the Variscan Belt of Europe and Circum-Atlantic Paleozoic Orogens* (edited by Matte, Ph.). *Tectonophysics* **177**, 81–107.

Dallmeyer, R. D. & Quesada, C. 1989. Geochronological contraints to the structural evolution of the Badajoz–Córdoba Shear Belt (Southeast Iberia). *Terra Abstracts* **1**, 366.

Dell'Angello, L. N. & Tullis, J. 1989. Fabric development in experimentally sheared quartzites. *Tectonophysics* **169**, 1–21.

Eguíluz, L. 1988. Petrogénesis de rocas ígneas y metamórficas en el Anticlinorio Burguillos-Monesterio, Macizo Ibérico Meridional. Unpublished thesis. Univ. País Vasco.

Eguíluz, L. & Abalos, B. 1992. Tectonic setting of Cadomian low-pressure metamorphism in the central Ossa–Morena Zone (Iberian Massif, SW Iberia). *Precambrian Res.* **56**, 113–137.

Etheridge, M. A. & Wilkie, J. C. 1981. An assessment of dynamically recrystallized grainsize as a paleopiezometer in quartz-bearing mylonite zones. *Tectonophysics* **78**, 475–508.

Galdeano, A., Miranda, J. M., Matte, Ph., Mouge, P. and Rossignol, C. 1990. Aeromagnetic data: a tool for studying the Variscan arc of western Europe and its correlations with transatlantic structures. In: *Terranes in the Variscan Belt of Europe and Circum-Atlantic Paleozoic Orogens* (edited by Matte, Ph.). *Tectonophysics* **177**, 293–305.

Gapais, D. & Barbarin, B. 1986. Quartz fabric transitions in a cooling syntectonic granite (Hermitage Massif, France). *Tectonophysics* **124**, 357–370.

Garbutt, J. N. & Teyssier, C. 1991. Prism ⟨*c*⟩ slip in the quartzites of the Dakhurst Mylonite Belt, California. *J. Struct. Geol.* **13**, 657–666.

García Casquero, J. L., Boelrijk, N. A. I. M., Chacón, J. & Priem, H. N. A. 1985. Rb–Sr evidence for presence of Ordovician granites in the deformed basement of the Badajoz–Cordoba belt, SW Spain. *Geol. Rdsch.* **74**, 379–384.

García Casquero, J. L., Boelrijk, N. A. I. M., Priem, H. N. A. & Chacón, J. 1988. Isotopic dating of the mylonitization of the Azuaga Group in the Badajoz-Córdoba belt, SW Spain. *Geol. Rdsch.* **77**, 483–489.

Gibbons, W. 1990. Transcurrent ductile shear zones and the dispersal of the Avalon superterrane. In: *The Cadomian Orogeny* (edited by D'Lemos, R. S., Strachan, R. A. & Topley, C. G.). *Spec. Publs geol. Soc. Lond.* **51**, 407–423.

Ighid, L., Saquaque, A. & Reuber, I. 1989. Plutons syn-cinématiques et la déformation panafricaine majeure dans le Saghro oriental (boutonnière d'Imiter, Anti-Atlas, Maroc). *C. r. Acad. Sci., Paris* **309**, 615–620.

Knipe, R. J. & Law, R. D. 1987. The influence of crystallographic orientation and grain-boundary migration on microstructural and textural evolution in a *S–C* mylonite. *Tectonophysics* **135**, 155–169.

Krohe, A. 1990. Local variations in quartz [*c*]-axis orientations in non-coaxial regimes and their significance for the mechanics of *S–C* fabrics. *J. Struct. Geol.* **12**, 995–1004.

Laurent, P. 1974. Structure et Pétrologie de la Bande Blastomylonitique de Badajoz–Córdoba a l'ouest d'Azuaga. Unpublished thése 3éme Cycle, Univ. Montpellier.

Le Fort, J. P. 1983. A new geophysical criterion to correlate the Acadian and Hercynian orogenies of western Europe and eastern America. *Mem. geol. Soc. Am.* **158**, 3–18.

Lister, G. S. & Snoke, A. W. 1984. S–C mylonites. *J. Struct. Geol.* **6**, 217–638.

Mainprice, D., Bouchez, J. L., Blumenfeld, Ph. & Tubía, J. M. 1986. Dominant -*c*- slip in naturally deformed quartz: implications for dramatic softening at high temperature. *Geology* **14**, 819–822.

Mancktelow, N. S. 1987. Quartz textures from the Simplon Fault Zone, southwest Switzerland and north Italy. *Tectonophysics* **135**, 133–153.

Mata, J. & Munhá, J. 1986. Geodynamic significance of high grade metamorphic rocks from Degolados-Campo Maior (Tomar–Badajoz–Córdoba Shear Zone). *Abstract. Maleo* **2**, 28.

Matte, Ph. 1991. Accretionary history and crustal evolution of the Variscan belt in Western Europe. In: *Accretionary Tectonics and Composite Continents* (edited by Hatcher, R. D. Jr & Zonenshain, L.). *Tectonophysics* **196**, 309–337.

Mercier, J. C., Anderson, D. A. & Carter, N. L. 1977. Stress in the lithosphere. Inferences from steady state flow of rocks. *Pure & Appl. Geophys.* **115**, 119–126.

Murphy, F. C. 1990. Basement-cover relationships of a reactivated Cadomian mylonite zone: Rosslare Complex, SE Ireland. In: *The Cadomian Orogeny* (edited by D'Lemos, R. S., Strachan, R. A. & Topley, C. G.). *Spec. Publs geol. Soc. Lond.* **51**, 329–339.

Murphy, J. B. & Nance, R. D. 1989. Model for the evolution of the Avalonian–Cadomian belt. *Geology* **17**, 735–738.

Murphy, J. B. & Nance, R. D. 1991. Supercontinent model for the contrasting character of Late Proterozoic orogenic belts. *Geology* **19**, 469–472.

Nance, R. D. 1990. Late Precambrian-Early Palaeozoic evolution of part of the Avalon terrane in southern New Brunswick, Canada. In: *The Cadomian Orogeny* (edited by D'Lemos, R. S., Strachan, R. A. & Topley, C. G.). *Specs. Publs geol. Soc. Lond.* **51**, 363–382.

Paris, F. & Robardet, M. 1977. Paléogéographie et relations ibéro-armoricaines au Paléozoique anté-carbonifère. *Bull. Soc. géol. Fr.* **19**, 1121–1126.

Passchier, C. W. & Simpson, C. 1986. Porphyroclast systems as kynematic indicators. *J. Struct. Geol.* **8**, 831–843.

Peacock, D. C. P. & Sanderson, D. J. 1991. Displacements, segment linkage and relay ramps in normal fault zones. *J. Struct. Geol.* **13**, 721–733.

Pfiffner, O. A. & Ramsay, J. G. 1982. Constraints on geological strain rates: arguments from finite strain states of naturally deformed rocks. *J. geophys. Res.* **87**, 311–321.

Quesada, C. 1990. Precambrian terranes in the Iberian Variscan Foldbelt. In: *Avalonian and Cadomian Geology of the North Atlantic* (edited by Strachan, R. A. & Taylor, G. K.). Blackie, New York, 109–133.

Quesada, C., Apalategui, O., Eguíluz, L., Liñán, E. & Palacios, T. 1990. Ossa–Morena Zone: Precambrian. In: *Pre-Mesozoic Geology of Iberia* (edited by Dallmeyer, R. D. & Martínez-García, E.). Springer, Berlin, 250–258.

Rabu, D., Chantraine, J., Chauvel, J. J., Denis, E., Balé, P. & Bardy, Ph. 1990. The Brioverian (Upper Proterozoic) and the Cadomian orogeny in the Armorican Massif. In: *The Cadomian Orogeny* (edited by D'Lemos, R. S., Strachan, R. A. & Topley, C. G.). *Spec. Publs geol. Soc. Lond.* **51**, 81–94.

Ramsay, J. G. 1967. *Folding and Fracturing of Rocks*. MacGraw-Hill, New York.

Schäfer, H. J. 1990. Geochronological investigations in the Ossa–Morena Zone, SW Spain. Unpublished Ph.D. thesis, Swiss Federal Institute of Technology.

Schäfer, H. J., Gebauer, D. & Nägler, Th.F. 1989. Pan-African and Caledonian ages in the Ossa–Morena Zone (Southwest Spain): a U–Pb zircon and Sm–Nd study. *Terra Abstracts* **1**, 350–351.

Schmid, S. M. & Casey, M. 1986. Complete fabric analysis of some commonly observed quartz *c*-axis patterns. In: *Mineral and Rock Deformation: Laboratory Studies—The Paterson Volume* (edited by Hobbs, B. E. & Heard, H. C.). *Am. Geophys. Un. Geophys. Monogr.* **36**, 263–286.

Sengör, A. M. C. 1991. Plate tectonics and orogenic research after 25 years: synopsis of a Tethyan perspective. *Tectonophysics* **187**, 315–344.

Simpson, C. & Schmid, S. M. 1983. An evaluation of criteria to deduce the sense of movement in sheared rocks. *Bull. geol. Soc. Am.* **94**, 1281–1288.

Strachan, R. A. & Roach, R. A. 1990. Tectonic evolution of the Cadomian Belt in north Brittany. In: *The Cadomian Orogeny* (edited by D'Lemos, R. S., Strachan, R. A. & Topley, C. G.). *Spec. Publs geol. Soc. Lond.* **51**, 133–150.

Stünitz, H. 1991. Folding and shear deformation in quartzites, inferred from crystallographic preferred orientation and shape fabrics. *J. Struct. Geol.* **13**, 71–86.

Treloar, P. J. & Strachan, R. A. 1990. Cadomian strike-slip tectonics in NE Brittany. In: *The Cadomian Orogeny* (edited by D'Lemos, R. S., Strachan, R. A. & Topley, C. G.). *Spec. Publs geol. Soc. Lond.* **51**, 151–168.

Twiss, R. J. 1977. Theory and applicability of a recrystallized grain size piezometer. *Pure & Appl. Geophys.* **115**, 227–244.

Vauchez, A. 1975. Tectoniques tangentielles superposées dans le segment hercynien sud-ibérique: les nappes et plis couchés de la region d'Alconchel-Fregenal de la Sierra (Badajoz). *Bol. Geol. Min.* **86**, 573–580.

Vauchez, A. & Nicolas, A. 1991. Mountain building: strike-parallel motion and mantle anisotropy. *Tectonophysics* **185**, 183–201.

Villeneuve, M., Bonvalot, S. & Alboux, Y. 1990. L'agencement des châines (pan-africaines et hercynienne) sur le bordure occidentale du craton ouest africain. *C. r. Acad. Sci., Paris* **310**, 955–962.

Wenk, H.-R., Canova, C., Molinari, A. & Rocks, V. F. 1989. Viscoplastic modeling of texture development in quartzite. *J. geophys. Res.* **94**, 17,895–17,906.

White, S. H. 1979. Paleostress estimates in the Moine Thrust zone. *Nature* **280**, 222–223.